TABLE 1: Expression of transgene in the mouse cochlea with vectors derived from the AAV1–4, 7, and 8 pseudotypes

Vector	Inner hair cells	Outer hair cells	Spiral ganglion	Stria vascularis	Spiral ligament	Spiral limbus	Reissner's membrane	Inner and outer pillar cells	Inner sulcus cells	Deiter's cells	Claudius' cells	Hensen's cells	Mesenchymal cells
AAV1	+++	−	++	−	++	++	++	−	+	−	−	−	++
AAV2	++	−	+	−	+	+	−	−	−	−	−	−	−
AAV3	++++	−	−	−	−	−	−	−	−	−	−	−	−
AAV4	−	−	−	−	−	−	−	−	−	−	−	−	+
AAV5	+++	−	+++	−	+	++	+	−	++	−	+	−	−
AAV7	+++	−	+	−	+++	++	−	−	+	−	+	−	++
AAV8	++++	−	−	−	+	+	−	−	++	−	+	−	+

The level of expression was graded by fluorescence intensity on a four-level scale (+, ++, +++, ++++) depending on the pixel/unit area count. ++++ means the strongest intensity of EGFP expression, + means the weakest intensity of EGFP expression, while − means no fluorescence.

was slowly infused into the scala tympani adjacent to the most basal turn of the cochlea. The percentage of transduced inner hair cells from the basal (high frequencies) to the apical (low frequencies) cochlear regions is shown in Fig. 4.

Cytotoxicity

We detected no deleterious effects on the viability of transduced cells. We compared evoked auditory brainstem response (ABR) threshold levels before and after injection, using a two-way repeated measure of the analysis of variance. There was no significant loss in ABR and hence no change in cochlear function for up to 10 days following vector infusion (Figs. 5A and 5B). In addition, the cellular and tissue architecture of experimental cochleae remained intact. There was no evidence of endolymphatic hydrops after AAV vector injection in any of the animals. We observed no significant destruction of the inner or outer hair cells (Fig. 5C).

Discussion

In the present study, we assessed the utility of vectors derived from seven AAV serotypes for gene delivery into the cochlea. Our results showed that the AAV3 vector was the most efficient and specific in transducing cochlear inner hair cells, although these cells could also be transduced with AAV1, 2, 5, 7, and 8 vectors. The transduction efficiency of the spiral ganglion by the AAV5 vector was particularly high, followed by that of the AAV1, AAV2, and AAV7 vectors. The efficient and specific transduction of inner hair cells with the AAV3 vector suggests that it recognizes a unique host range with a distinct cellular receptor. Transduction efficiency is dependent on initial viral binding (a property of the viral capsid), entry, and various postentry processes such as intracellular trafficking and second-strand synthesis [20–22]. The genome size of AAV vectors has also been demonstrated to affect transduction efficiency [23]. Comparisons of the serotypes have indicated that heterogeneity in the capsid-encoding regions and a differential ability to transduce cells may be associated with different receptor and co-receptor requirements for cell entry [24]. However, the receptors and co-receptors of AAV3 have not yet been clearly identified.

In the current study, we found that cochlear inner hair cells could be transduced with six AAV serotypes, although Lalwini *et al.* [8] reported that outer hair cells could be transduced with a low titer (1×10^6 viral particles/ml) of AAV2 *in vivo*. After injecting the AAV2 vector, we found that the spiral ganglion neurons, the inner hair cells, and the cells in the spiral ligament were all transduced. This transduction pattern differs from that reported in previous studies [8,10,17], and this discrepancy might be due to the different delivery methods and dissimilar promoters. Although the CAG promoter directs

doi:10.1016/j.ymthe.2005.03.021

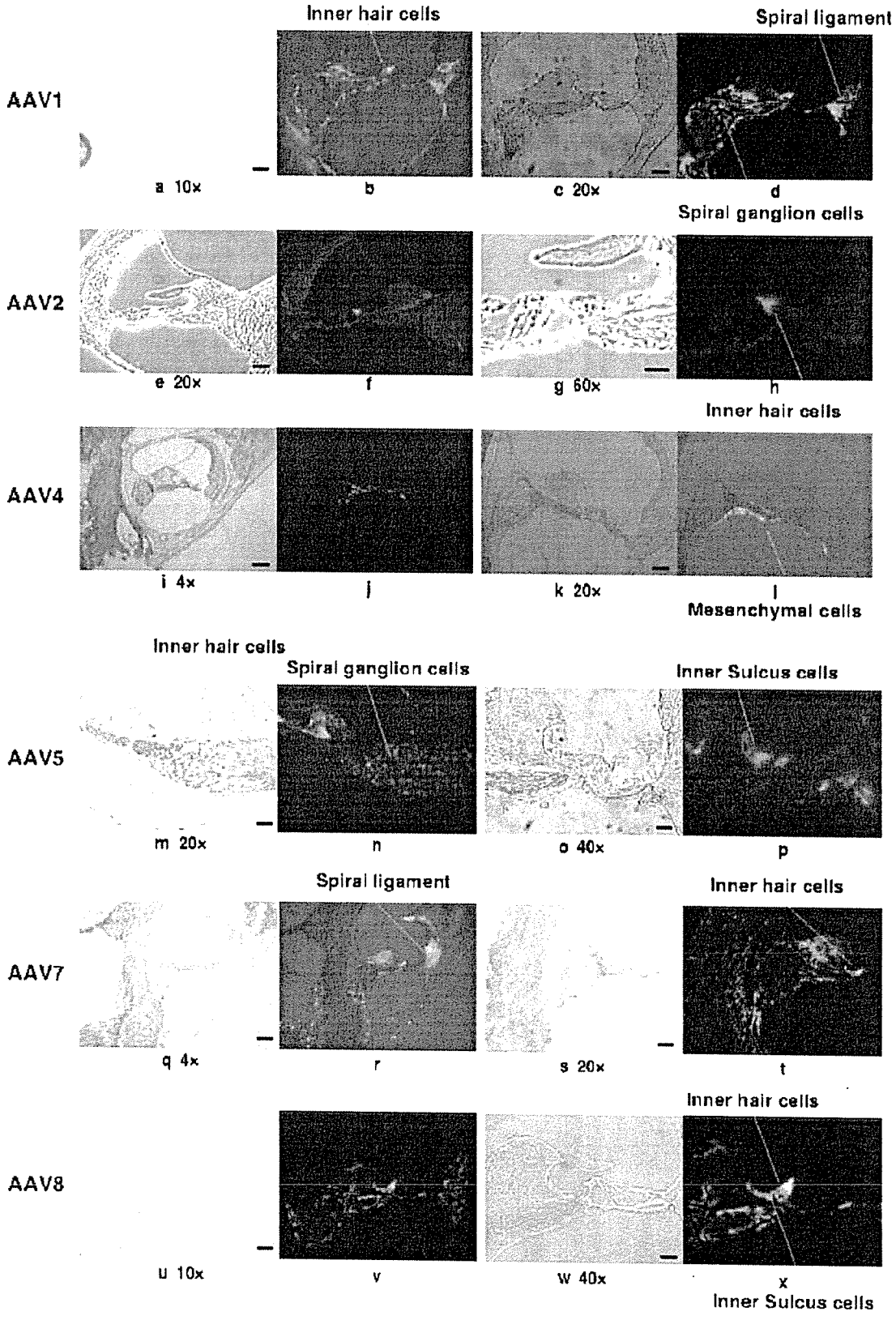

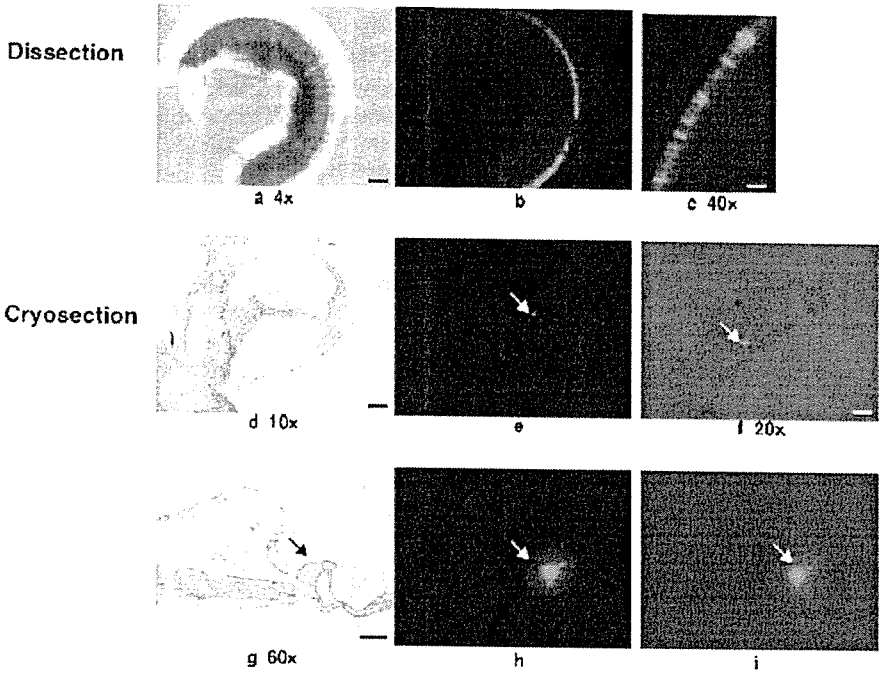

FIG. 3. Cochlear transduction with AAV3-CAG-EGFP. Dissected cochleae and cryosections show transgene expression in inner hair cells. (a) A light photomicrograph of the basal turn of the cochlea is shown, illustrating its laminar structure. (b) A fluorescence photomicrograph of this dissection. (c) A higher magnification view of the dissection shown in (b), illustrating a row of inner hair cells in the organ of Corti expressing EGFP. (d–i) Representative photomicrographs from three magnifications of a radial cochlear cryosection. (d) Light photomicrography of an intact cochlear duct. Fluorescence photomicrography of this duct is shown in (e). (h and i) A higher magnification of (e), illustrating EGFP expression within inner hair cells. Cryosections show transgene expression in the inner hair cells (arrows). Scale bars: 4×, 250 μm; 10×, 100 μm; 20×, 50 μm; 40×, 25 μm; 60×, 25 μm.

higher expression than do the cytomegalovirus (CMV) and EF-1α promoters [25], each promoter drives reporter gene expression in different cell types [26,27].

Cell-specific or -selective infectivity of the viral vectors suggests the presence of various factors to introduce the distinct expression patterns of the transgenes. Spiral ganglion neurons and glial cells can be transduced with a lentivirus–GFP construct *in vitro* but not *in vivo* [7]. The differential transducibility under *in vivo* and *in vitro* conditions reflects a high degree of structural isolation of the spiral ganglion and other cell types—such as the cells on the periphery of the endolymph—from the perilymph into which the viral vector was introduced. The strict separation of the endolymph from the perilymph is maintained by tight junctions that line the boundary between these fluid chambers. The size of the viral particle may contribute to the observed variability in transgene expression promoted by different vectors. The diameters of adenovirus and retrovirus (including lentivirus) particles are approximately 75 nm and greater than 100 nm, respectively, while the diameters of AAV vectors are typically 11–22 nm [28,29]. Thus, the larger size of lentiviruses and adenoviruses may limit their subsequent dissemination from the perilymph into the endolymph. The variable patterns of adenovirus- and lentivirus-mediated gene expression seen with different methods of inoculation may be due to the inoculation route, the volume and number of viral particles, differences in viral preparation, or differences in the method of transgene detection. The introduction of adenovirus vectors by cochleostomy or with an osmotic pump via the round window leads to a more efficient transduction of cochlear hair cells [30–32]. The apical domain (apical membrane and stereocilia) of cells in the sensory epithelium (hair cells and supporting cells) is bathed in endolymph, while the basal–lateral domain is immersed in perilymph. Access of the viral vectors to the endolymphatic space by cochleostomy may facilitate the transduction of hair cells and supporting cells. However, although the cochleostomy procedure has been tested, inoculation into the membranous labyrinth could not be confirmed [32]. In the present study, AAV vectors were found to infect cochlear hair cells easily *in vivo,* via round window injection.

Gene transfer into the cochlea through the round window membrane is ideal, because this procedure

FIG. 2. Transduction of the cochleae by AAV1-, AAV2-, AAV4-, AAV5-, AAV7-, and AAV8-based vectors. (a, c, e, g, i, k, m, o, q, s, u, and w) Light photomicrographs of cochlear cryosections. (b, d, f, h, j, l, n, p, r, t, v, and x) Fluorescence photomicrographs (green fluorescence from transgene). The spiral ligament cells were transduced prominently with the AAV1 and AAV7 vectors (d and r). Transgene expression in inner hair cells was detected with AAV1-, AAV2-, AAV5-, AAV7-, and AAV8-based vectors (b, h, n, t, and x). AAV4-based vector faintly transduced mesenchymal cells (j and l). The spiral ganglion cells showed significant levels of fluorescence with the AAV5-based vector (n). Intense fluorescence was detected with the AAV5- and AAV8-based vectors in the inner sulcus cells (p and x). Scale bars: 10×, 100 μm; 20×, 50 μm; 40×, 25 μm; 60×, 25 μm.

doi:10.1016/j.ymthe.2005.03.021

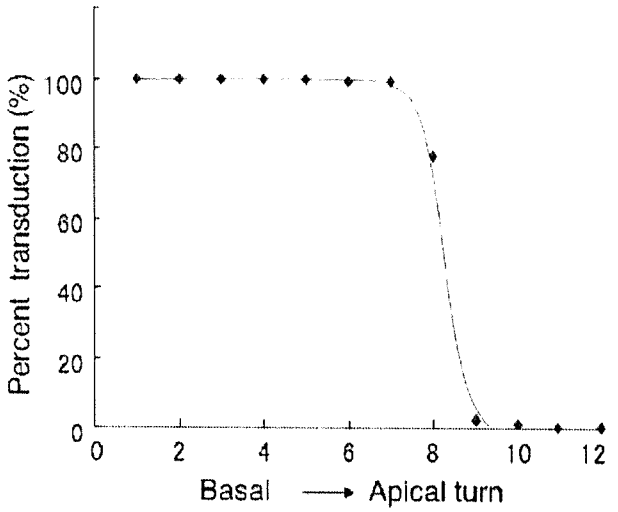

FIG. 4. EGFP expression profile of inner hair cells transduced with AAV3, as shown for a cross section subdivided into 12 segments ranging from the basal (high frequencies) to the apical (low frequencies) cochlear regions.

requires simple surgery without cochlear trauma [19]. Another critical factor in assessing the utility of a gene transfer vector is safety. Factors determining safety include the toxicity of the gene transfer agent itself, the provocation of immune responses, the generation of replication-competent virus, and the risk of creating genetically modified cells by insertional mutagenesis. The cells and tissues within the AAV-EGFP-perfused cochleae were free from inflammation and were generally intact. No pathological changes were observed in the organ of Corti, stria vascularis, or spiral ganglion cells. The long-term expression of EGFP within the cochlear tissues is consistent with data obtained from other animal models and different organ systems [9,33]. Since EGFP is known to introduce cellular toxicity, vectors expressing physiologically therapeutic proteins would achieve longer transduction periods than EGFP. Gene transfer into the inner hair cells presents numerous opportunities for auditory neuroscience. Potential applications include the localization of proteins by expression of tagged constructs, the generation of dominant-negative or antisense knockouts of endogenous proteins, the rescue of mutant phenotypes to identify disease genes, and perhaps even the treatment of auditory disorders. Advances in the molecular basis of auditory diseases have allowed the identification of a number of genetic disorders such as presbycusis, acoustic trauma, and ototoxicity. The development of gene therapy now allows us to evaluate the effects of transferring therapeutic genes into the inner ear by several different strategies. The expression of marker genes in the inner ear tissue has been demonstrated. Further studies will improve our understanding of cochlear function as well as provide for the development of novel therapies for a wide variety of inner ear diseases. Intracochlear gene transfer using AAV vectors has been established as a viable experimental proposition. Future study will include the transfer of functioning genes *in vivo* and the development of alternative vectors. While clinical application may be some way off, it is vital that gene delivery techniques are optimized in anticipation of future need.

In conclusion, the data presented in this paper demonstrate successful gene transfer into several types of cochlear cells *in vivo* with AAV-based vectors. Interestingly, the AAV3 vector promoted inner hair cell-specific transduction. These findings are of value for further molecular studies of the cochlear inner hair cells and for gene replacement strategies to correct hereditary hearing loss due to specific monogenic mutations affecting cochlear inner hair cells.

MATERIALS AND METHODS

Construction and preparation of proviral plasmids. The AAV vector proviral plasmid pAAV2-*LacZ* harbors an *Escherichia coli* β-galactosidase expression cassette with the CMV promoter, the first intron of the human growth hormone gene, and the SV40 early polyadenylation sequence, which are flanked by inverted terminal repeats (ITRs) [34]. The *LacZ* expression cassette of pAAV2-*LacZ* was ligated to *Not*I-excised pAAV5-RNL [35] to form the proviral plasmid pAAV5-*LacZ*. The pAAV2-CAG-EGFP-WPRE construct consists of the EGFP gene under the control of the CAG promoter (the chicken β-actin promoter associated with the cytomegalovirus immediate-early enhancer) and WPRE (woodchuck hepatitis virus posttranscriptional regulatory element) flanked by ITRs. The WPRE cassette augments the stability of transgene mRNA [36] and increases EGFP expression levels, thereby ensuring long-term transgene expression. A *Bam*HI–*Xba*I fragment containing the EGFP cDNA excised from pEGFP-1 and a *Hin*dIII fragment containing the WPRE sequence excised from pBS II SK$^+$WPRE-B11 (a gift from Dr. J. Donello) was ligated to *Xho*I linkers and cloned into an *Xho*I site of pCAGGS (a gift from Dr. J.-I. Miyazaki) to create pCAG-EGFP-WPRE. The EGFP expression cassette from pCAG-EGFP-WPRE was ligated to the *Not*I-excised pAAV2-*LacZ* and pAAV5-RNL [35] to form the proviral plasmids pAAV2-CAG-EGFP-WPRE and pAAV5-CAG-EGFP-WPRE, respectively. The AAV-helper plasmid harbors Rep and Cap. The adenovirus helper plasmid pAdeno5 (identical to pVAE2AE4-5) encodes the entire E2A and E4 regions and the VA RNA I and II genes [37]. Plasmids were purified with the Qiagen plasmid purification kits (Qiagen K.K., Tokyo, Japan).

Recombinant AAV vector production. Vectors derived from the AAV1–4, 7, and 8 pseudotypes were produced with the AAV packaging plasmid pAAV1RepCap (for AAV1) [38], pHLP19 (for AAV2), pAAV3RepCap (for AAV3) [39], pAAV4RepCap (for AAV4) [40], pAAV7RepCap (for AAV7) [41], or pAAV8RepCap (for AAV8) [41] and the AAV proviral plasmid pAAV2-*LacZ* or pAAV2-CAG-EGFP-WPRE. The plasmids pAAV5RepCap [35] and pAAV5-*LacZ*, or pAAV5-CAG-EGFP-WPRE, were used to produce vector with the AAV5 pseudotype [42]. Seven AAV serotype vectors were produced as previously described by the three-plasmid transfection adenovirus-free protocol [37]. Briefly, three days before transfection, 293 cells were plated onto a 10-tray Cell Factory (Nalge Nunc International, Rochester, NY, USA; 6×10^7 cells/10-tray). The cells were cotransfected with 650 μg each of the proviral plasmid, the AAV vector packaging plasmid, and the adenovirus helper plasmid pAdeno5 [34] by the calcium phosphate coprecipitation method. The medium was changed following incubation for 6–8 h at 37°C. Recombinant AAV was harvested 72 h after transfection by three freeze/thaw cycles. The crude viral lysate was purified twice on a cesium chloride two-tier centrifugation

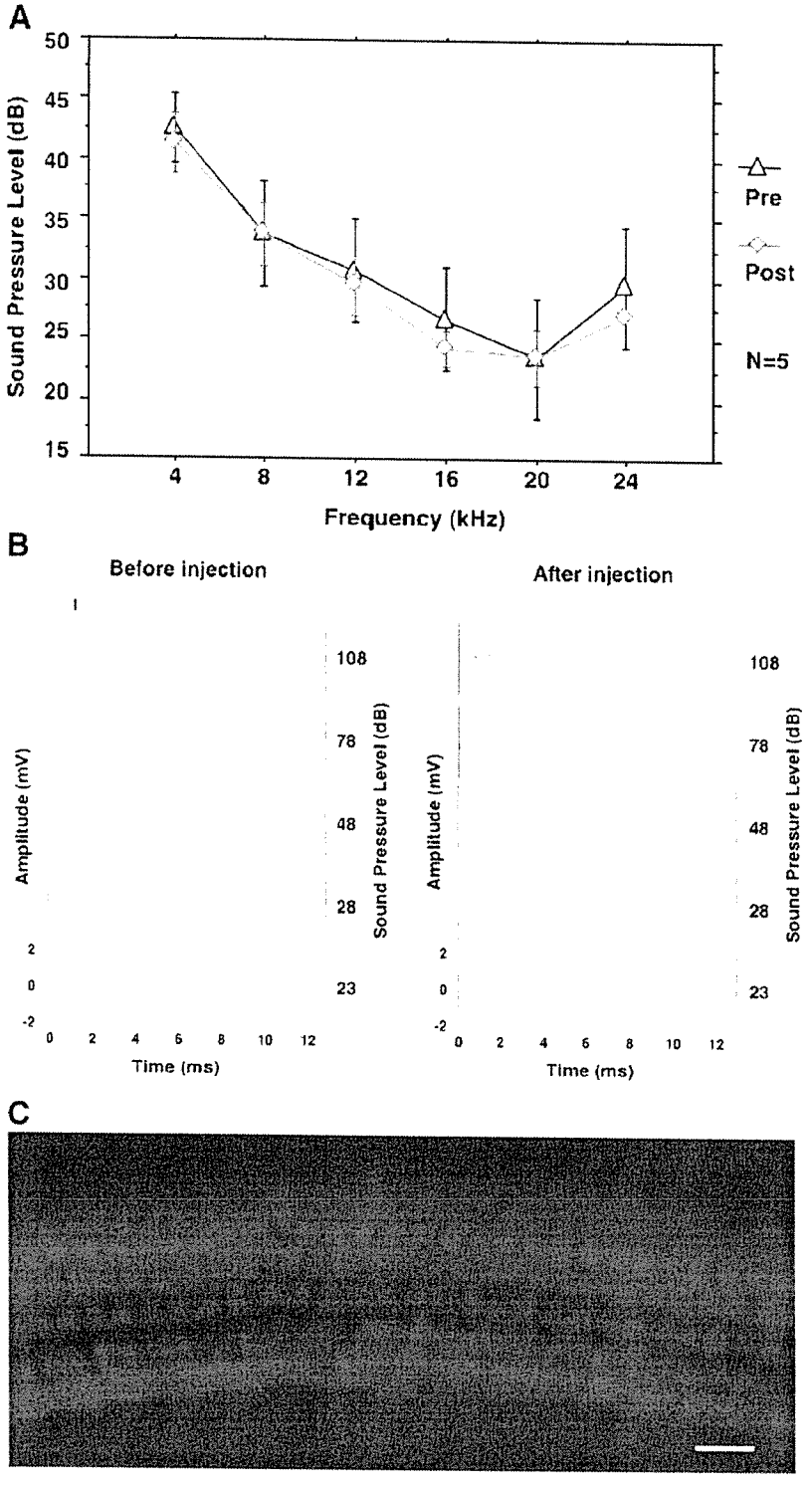

FIG. 5. (A) ABR threshold (mean ± SD) at each frequency tested preoperatively (pre) versus postoperatively (post). (B) Example of ABR waveforms in C57BL/6J at various stimuli (16 kHz; 108 dB, 78 dB, 48 dB, 28 dB, and 23 dB). ABR were tested in the transduced ear prior to viral injection and 10 days after injection. Wave I was measured to analyze the activity of the cochlea. (C) F-actin staining showing that no outer hair cells were lost from inoculated cochleae. Original magnification 40×; scale bar, 25 μm.

gradient as described previously [24]. The viral stock was treated with DNase and titrated by quantitative real-time PCR with plasmid standards [43].

Surgical procedures and cochlear perfusions. All animal studies were performed in accordance with the guidelines issued by the committee on animal research of Jichi Medical School and approved by its ethics

doi:10.1016/j.ymthe.2005.03.021

committee. Sixty female C57BL/6J mice (4 weeks of age; CLEA Japan, Tokyo, Japan) and 40 male ICR mice (2 months of age; Japan SLC, Shizuoka, Japan) were utilized. The mice were initially anesthetized with ketamine (50 mg/kg) and the analgesic xylazine (5 mg/kg). A postauricular approach was used to expose the tympanic bony bulla. A small opening (2 mm) in the tympanic bulla was carefully made to allow access to the round window membrane. In the tested groups, 5 μl AAV vector solution (5×10^{10} gc) was microinjected into the cochlea through the round window over 10 min with a glass micropipette (40 μm in diameter) fitted on a Univentor 801 syringe pump (Serial No. 170182, High Precision Instruments, Univentor Ltd., Malta) [19]. A small plug of muscle was used to seal the cochlea and the surgical wound was closed in layers and dressed with antibiotic ointment. Five mice of each strain received control cochlear perfusions with artificial perilymph (145 mM NaCl, 2.7 mM KCl, 2 mM $MgSO_4$, 1.2 mM $CaCl_2$, 5 mM Hepes) alone. Each AAV-EGFP serotype was injected into five mice of each strain. Another 20 C57BL/6J mice were injected with the AAV3 vector to study long-term expression.

Cochlear function assessment using ABR. To assess the physiological status of experimental ears, auditory thresholds were determined with multiple frequency and intensity tone bursts by performing ABR audiometry with Tucker–Davis Technologies and Scope v3.6.9 software (Power Lab/200; ADInstruments, Castle Hill, Australia). Tone pipes were introduced into the operated ears of the anesthetized mice, and evoked potentials were recorded using needle electrodes inserted through the skin. ABR were elicited and measured 256 times at 4, 8, 12, 16, 20, and 24 kHz frequencies with tone bursts in systematic 5-dB steps. The rise/fall times for the tone bursts were 0.1 ms rise/ms flat (cosine gate). Free-field system was used as a calibration procedure. Wave I was measured to analyze the activity from the cochlea. The lowest stimulus level that yielded a detectable ABR waveform was defined as the threshold. ABR were tested in the infused ear prior to surgery and 10 days postsurgery. Data were statistically analyzed using repeated-measures analysis of variance followed by paired Student's t test performed with StatView 5.0 software (SAS Institute Inc., Cary, NC, USA). Values of $P < 0.05$ were considered significant.

Histology. Cochlear transgene expression patterns were determined for all AAV serotypes by visualizing EGFP expression. The animals were sacrificed 10 days after injection, and intracardiac perfusion was performed with 4% paraformaldehyde (PFA) in 0.1 M phosphate buffer, pH 7.4. The cochleae were harvested and the stapes footplates were removed. For AAV3-mediated transduction, the animals (five mice for each time point) were sacrificed 1, 2, 4, 8, or 12 weeks after inoculation. Postfixation was carried out in 4% PFA for 4 h at 4°C, and decalcification was performed in 10% EDTA for 12 days at room temperature. The cochlear half-turns were microdissected and processed and the other half-turns were prepared by cryosection (10 μm) to detect EGFP expression by using an Olympus IX70 (Olympus Corp., Tokyo, Japan) fluorescence microscope with a standard fluorescein isothiocyanate filter set and Studio Lite software (Olympus Corp.). Cells that exhibited fluorescence were considered positive for transgene expression. The level of expression was graded by fluorescence intensity on a four-point scale (+, ++, +++, ++++) depending on the pixel/unit area count. Hair cell counts were carried out with dissected cochlea.

ACKNOWLEDGMENTS

The authors thank Avigen, Inc. (Alameda, CA, USA) for providing pAAV-LacZ, pHLP19, and pAdeno; Dr. John A. Chiorini for pAAV4RepCap (identical to pSV40oriAAV4-2), pAAV5-RNL, and pAAV5RepCap (identical to 5RepCapB); and Dr. James M. Wilson for pAAV7RepCap and pAAV8RepCap. We also thank Dr. John E. Donello (Infectious Disease Laboratory, The Salk Institute for Biological Studies) for providing pBS II SK+WPRE-B11 and Dr. Jun-Ichi Miyazaki (Osaka University Graduate School of Medicine) for pCAGGS. The authors also thank Mr. Takeshi Hayakawa (Bio Research Center Co., Ltd.), Ms. Miyoko Mitsu, and Ms. Kiyomi Aoki for their encouragement and technical support. This study was supported in part by (1) grants from the Ministry of Health, Labor, and Welfare of Japan; (2) Grants-in-Aid for Scientific Research; (3) a grant from the 21 Century COE Program; and (4) the High-Tech Research Center Project for Private Universities matching fund subsidy from the Ministry of Education, Culture, Sports, Science, and Technology of Japan.

RECEIVED FOR PUBLICATION NOVEMBER 1, 2004; ACCEPTED MARCH 24, 2005.

REFERENCES

1. Raphael, Y., Frisancho, J. C., and Roessler, B. J. (1996). Adenoviral-mediated gene transfer into guinea pig cochlear cells in vivo. *Neurosci. Lett.* **207:** 137–141.
2. Holt, J. R., *et al.* (1999). Functional expression of exogenous proteins in mammalian sensory hair cells infected with adenoviral vectors. *J. Neurophysiol.* **81:** 1881–1888.
3. Yamasoba, T., Suzuki, M., and Kondo, K. (2002). Transgene expression in mature guinea pig cochlear cells in vitro. *Neurosci. Lett.* **335:** 13–16.
4. Derby, M. L., Sena-Esteves, M., Breakefield, X. O., and Corey, D. P. (1999). Gene transfer into the mammalian inner ear using HSV-1 and vaccinia virus vectors. *Hear. Res.* **134:** 1–8.
5. Chen, X., Frisina, R. D., Bowers, W. J., Frisina, D. R., and Federoff, H. J. (2001). HSV amplicon-mediated neurotrophin-3 expression protects murine spiral ganglion neurons from cisplatin-induced damage. *Mol. Ther.* **3:** 958–963.
6. Bowers, W. J., Chen, X., Guo, H., Frisina, D. R., Federoff, H. J., and Frisina, R. D. (2002). Neurotrophin-3 transduction attenuates cisplatin spiral ganglion neuron ototoxicity in the cochlea. *Mol. Ther.* **6:** 12–18.
7. Han, J. J., *et al.* (1999). Transgene expression in the guinea pig cochlea mediated by a lentivirus-derived gene transfer vector. *Hum. Gene Ther.* **10:** 1867–1873.
8. Lalwani, A. K., Walsh, B. J., Reilly, P. G., Muzyczka, N., and Mhatre, A. N. (1996). Development of in vivo gene therapy for hearing disorders: introduction of adeno-associated virus into the cochlea of the guinea pig. *Gene Ther.* **3:** 588–592.
9. Lalwani, A., *et al.* (1998). Long-term in vivo cochlear transgene expression mediated by recombinant adeno-associated virus. *Gene Ther.* **5:** 277–281.
10. Luebke, A. E., Foster, P. K., Muller, C. D., and Peel, A. L. (2001). Cochlear function and transgene expression in the guinea pig cochlea, using adenovirus- and adeno-associated virus-directed gene transfer. *Hum. Gene Ther.* **12:** 773–781.
11. Luebke, A. E., Steiger, J. D., Hodges, B. L., and Amalfitano, A. (2001). A modified adenovirus can transfect cochlear hair cells in vivo without compromising cochlear function. *Gene Ther.* **8:** 789–794.
12. Staecker, H., Li, D., O'Malley, B. W., Jr., and Van De Water, T. R. (2001). Gene expression in the mammalian cochlea: a study of multiple vector systems. *Acta Otolaryngol.* **121:** 157–163.
13. Dazert, S., Aletsee, C., Brors, D., Gravel, C., Sendtner, M., and Ryan, A. (2001). In vivo adenoviral transduction of the neonatal rat cochlea and middle ear. *Hear. Res.* **151:** 30–40.
14. Ishimoto, S., Kawamoto, K., Kanzaki, S., and Raphael, Y. (2002). Gene transfer into supporting cells of the organ of Corti. *Hear. Res.* **173:** 187–197.
15. Van de Water, T. R., Staecker, H., Halterman, M. W., and Federoff, H. J. (1999). Gene therapy in the inner ear: mechanisms and clinical implications. *Ann. N.Y. Acad. Sci.* **884:** 345–360.
16. Vassalli, G., Bueler, H., Dudler, J., von Segesser, L. K., and Kappenberger, L. (2003). Adeno-associated virus (AAV) vectors achieve prolonged transgene expression in mouse myocardium and arteries in vivo: a comparative study with adenovirus vectors. *Int. J. Cardiol.* **90:** 229–238.
17. Li Duan, M., Bordet, T., Mezzina, M., Kahn, A., and Ulfendahl, M. (2002). Adenoviral and adeno-associated viral vector mediated gene transfer in the guinea pig cochlea. *Neuroreport* **13:** 1295–1299.
18. Lalwani, A. K., Han, J. J., Walsh, B. J., Zolotukhin, S., Muzyczka, N., and Mhatre, A. N. (1997). Green fluorescent protein as a reporter for gene transfer studies in the cochlea. *Hear. Res.* **114:** 139–147.
19. Kho, S. T., Pettis, R. M., Mhatre, A. N., and Lalwani, A. K. (2000). Cochlear microinjection and its effects upon auditory function in the guinea pig. *Eur. Arch. Otorhinolaryngol.* **257:** 469–472.
20. Handa, A., Muramatsu, S., Qiu, J., Mizukami, H., and Brown, K. E. (2000). Adeno-associated virus (AAV)-3-based vectors transduce haematopoietic cells not susceptible to transduction with AAV-2-based vectors. *J. Gen. Virol.* **81:** 2077–2084.
21. Davidson, B. L., *et al.* (2000). Recombinant adeno-associated virus type 2, 4, and 5 vectors: transduction of variant cell types and regions in the mammalian central nervous system. *Proc. Natl. Acad. Sci. USA* **97:** 3428–3432.
22. Zabner, J., *et al.* (2000). Adeno-associated virus type 5 (AAV5) but not AAV2 binds to the apical surfaces of airway epithelia and facilitates gene transfer. *J. Virol.* **74:** 3852–3858.
23. Yang, G. S., *et al.* (2002). Virus-mediated transduction of murine retina with adeno-associated virus: effects of viral capsid and genome size. *J. Virol.* **76:** 7651–7660.
24. Okada, T., *et al.* (2002). Adeno-associated virus vectors for gene transfer to the brain. *Methods* **28:** 237–247.
25. Xu, L., *et al.* (2001). CMV-beta-actin promoter directs higher expression from an

adeno-associated viral vector in the liver than the cytomegalovirus or elongation factor 1 alpha promoter and results in therapeutic levels of human factor X in mice. *Hum. Gene Ther.* **12:** 563–573.
26. Chung, S., Andersson, T., Sonntag, K. C., Bjorklund, L., Isacson, O., and Kim, K. S. (2002). Analysis of different promoter systems for efficient transgene expression in mouse embryonic stem cell lines. *Stem Cells* **20:** 139–145.
27. Nomoto, T., *et al.* (2003). Distinct patterns of gene transfer to gerbil hippocampus with recombinant adeno-associated virus type 2 and 5. *Neurosci. Lett.* **340:** 153–157.
28. Dutta, S. K. (1975). Isolation and characterization of an adenovirus and isolation of its adenovirus-associated virus in cell culture from foals with respiratory tract disease. *Am. J. Vet. Res.* **36:** 247–250.
29. Palmer, E., and Goldsmith, C. S. (1988). Ultrastructure of human retroviruses. *J. Electron Microsc. Tech.* **8:** 3–15.
30. Stover, T., Yagi, M., and Raphael, Y. (1999). Cochlear gene transfer: round window versus cochleostomy inoculation. *Hear. Res.* **136:** 124–130.
31. Stover, T., Yagi, M., and Raphael, Y. (2000). Transduction of the contralateral ear after adenovirus-mediated cochlear gene transfer: round window versus cochleostomy inoculation. *Gene Ther.* **7:** 377–383.
32. Kawamoto, K., Oh, S. H., Kanzaki, S., Brown, N., and Raphael, Y. (2001). The functional and structural outcome of inner ear gene transfer via the vestibular and cochlear fluids in mice. *Mol. Ther.* **4:** 575–585.
33. Kaplitt, M. G., *et al.* (1994). Long-term gene expression and phenotypic correction using adeno-associated virus vectors in the mammalian brain. *Nat. Genet.* **8:** 148–154.
34. Okada, T., *et al.* (2001). Development and characterization of an antisense-mediated prepackaging cell line for adeno-associated virus vector production. *Biochem. Biophys. Res. Commun.* **288:** 62–68.
35. Chiorini, J. A., Kim, F., Yang, L., and Kotin, R. M. (1999). Cloning and characterization of adeno-associated virus type 5. *J. Virol.* **73:** 1309–1319.
36. Zufferey, R., Donello, J. E., Trono, D., and Hope, T. J. (1999). Woodchuck hepatitis virus posttranscriptional regulatory element enhances expression of transgenes delivered by retroviral vectors. *J. Virol.* **73:** 2886–2892.
37. Matsushita, T., *et al.* (1998). Adeno-associated virus vectors can be efficiently produced without helper virus. *Gene Ther.* **5:** 938–945.
38. Mochizuki, S., *et al.* (2004). Adeno-associated virus (AAV) vector-mediated liver- and muscle-directed transgene expression using various kinds of promoters and serotypes. *Gene Ther. Mol. Biol.* **8:** 9–18.
39. Muramatsu, S., Mizukami, H., Young, N. S., and Brown, K. E. (1996). Nucleotide sequencing and generation of an infectious clone of adeno-associated virus 3. *Virology* **221:** 208–217.
40. Chiorini, J. A., Yang, L., Liu, Y., Safer, B., and Kotin, R. M. (1997). Cloning of adeno-associated virus type 4 (AAV4) and generation of recombinant AAV4 particles. *J. Virol.* **71:** 6823–6833.
41. Gao, G. P., Alvira, M. R., Wang, L., Calcedo, R., Johnston, J., and Wilson, J. M. (2002). Novel adeno-associated viruses from rhesus monkeys as vectors for human gene therapy. *Proc. Natl. Acad. Sci. USA* **99:** 11854–11859.
42. Rabinowitz, J. E., *et al.* (2002). Cross-packaging of a single adeno-associated virus (AAV) type 2 vector genome into multiple AAV serotypes enables transduction with broad specificity. *J. Virol.* **76:** 791–801.
43. Veldwijk, M. R., *et al.* (2002). Development and optimization of a real-time quantitative PCR-based method for the titration of AAV-2 vector stocks. *Mol. Ther.* **6:** 272–278.
44. Kikuchi, T., *et al.* (1995). *Anat. Embryol. (Berlin)* **191:** 101–118.

ARTICLE

doi:10.1016/j.ymthe.2005.08.009

Viral-Mediated Temporally Controlled Dopamine Production in a Rat Model of Parkinson Disease

Xiao-gang Li,[1,2] Takashi Okada,[2] Mika Kodera,[1] Yuko Nara,[1] Naomi Takino,[1] Chieko Muramatsu,[1] Kunihiko Ikeguchi,[1] Fumi Urano,[3] Hiroshi Ichinose,[3] Daniel Metzger,[4] Pierre Chambon,[4] Imaharu Nakano,[1] Keiya Ozawa,[2,*] and Shin-ichi Muramatsu[1,†]

[1]*Division of Neurology, Department of Medicine, and* [2]*Divison of Genetic Therapeutics, Center for Molecular Medicine, Jichi Medical School, Tochigi 329-0498, Japan*

[3]*Department of Life Science, Tokyo Institute of Technology, Kanagawa 226-8501, Japan*

[4]*Institut de Génétique et de Biologie Moléculaire et Cellulaire, Centre National de la Recherche Scientifique, Institut National de la Santé et de la Recherche Médicale, Université Louis Pasteur, Collège de France, and Institut Clinique de la Souris, 67404 Illkirch Cedex, France*

*To whom correspondence and reprint requests should be addressed at the Division of Genetic Therapeutics, Center for Molecular Medicine, Jichi Medical School, 3311-1 Yakushiji, Minamikawachi, Tochigi 329-0498, Japan. Fax: +81 285 44 8675. E-mail: kozawa@ms.jichi.ac.jp.

†To whom correspondence and reprint requests should be addressed at the Division of Neurology, Department of Medicine, Jichi Medical School, 3311-1 Yakushiji, Minamikawachi, Tochigi 329-0498, Japan. Fax: +81 285 44 5118. E-mail: muramats@ms.jichi.ac.jp.

Available online 22 September 2005

Regulation of gene expression is necessary to avoid possible adverse effects of gene therapy due to excess synthesis of transgene products. To reduce transgene expression, we developed a viral vector-mediated somatic regulation system using inducible Cre recombinase. A recombinant adeno-associated virus (AAV) vector expressing Cre recombinase fused to a mutated ligand-binding domain of the estrogen receptor α (CreER^{T2}) was delivered along with AAV vectors expressing dopamine-synthesizing enzymes to rats of a Parkinson disease model. Treatment with 4-hydroxytamoxifen, a synthetic estrogen receptor modulator, activated Cre recombinase within the transduced neurons and induced selective excision of the tyrosine hydroxylase (TH) coding sequence flanked by loxP sites, leading to a reduction in transgene-mediated dopamine synthesis. Using this strategy, aromatic L-amino acid decarboxylase (AADC) activity was retained so that L-3,4-dihydroxyphenylalanine (L-dopa), a substrate for AADC, could be converted to dopamine in the striatum and the therapeutic effects of L-dopa preserved, even after reduction of TH expression in the case of dopamine overproduction. Our data demonstrate that viral vector-mediated inducible Cre recombinase can serve as an *in vivo* molecular switch, allowing spatial and temporal control of transgene expression, thereby potentially increasing the safety of gene therapy.

Key Words: adeno-associated virus, gene therapy, gene regulation, tamoxifen, Cre recombinase, Parkinson disease, dopamine

INTRODUCTION

Advances in gene transfer methods, in particular the development of improved viral vectors, have expanded the potential of gene therapy to treat a wide range of genetic and acquired diseases. Efficient and long-term expression of therapeutic genes within the central nervous system has been demonstrated in preclinical studies aimed at treating neurodegenerative disorders, including Parkinson disease (PD) [1,2]. PD is a progressive movement disorder characterized by selective degeneration of dopaminergic neurons within the substantia nigra, which project to the striatum. As the dopamine content of the striatum decreases severely, its replacement becomes an important strategy to alleviate motor impairment of the disease. One such strategy is gene therapy to restore the local production of dopamine. Recombinant adeno-associated virus (AAV) vector-mediated gene transfer of dopamine-synthesizing enzymes, such as tyrosine hydroxylase (TH) and guanosine triphosphate cyclohydrolase I (GCH), with or without aromatic L-amino acid decarboxylase (AADC), has induced behavioral recovery in animal models of PD [3–5]. Before clinical trials examining this therapy can commence, however, it is desirable to have a mechanism by which

1525-0016/$30.00

dopamine synthesis can be controlled by regulation of gene expression.

Methods utilizing the properties of bacteriophage P1 site-specific Cre recombinase have been developed in recent years as a means of generating somatic mutations [6]. Regulation of Cre recombinase activity, achieved by fusing Cre with mutated hormone-binding domains of various steroid receptors, has been used in various transgenic applications [7,8]. A chimeric protein known as CreER^{T2}, obtained by fusing Cre to a mutated ligand binding domain of the human estrogen receptor α, is particularly useful. Cell-specific expression of CreER^{T2} in transgenic mice allows efficient tamoxifen-dependent Cre-mediated recombination at loci flanked by loxP sites, without background activity [9]. In the present study, we demonstrate that stereotaxic injection of recombinant AAV vectors expressing dopamine-synthesizing enzymes and CreER^{T2} enables spatiotemporal control of dopamine levels within the brains of rats of a PD model. Our results indicate that these vectors may have a number of applications in gene therapy.

RESULTS

Viral-Mediated Temporally Controlled Cre-Mediated Recombination

We generated AAV vectors expressing either Cre recombinase containing a nuclear localization signal (AAV-Cre) or tamoxifen-dependent Cre recombinase (AAV-CreER^{T2}). To engineer a reporter system, we designed an AAV-EGFP/Red vector to express a destabilized variant of red fluorescent protein (DsRed-Express DR) only after Cre-mediated recombination of a loxP-flanked DNA segment encoding a destabilized, red-shifted variant of green fluorescent protein (d2EGFP) (Fig. 1A). To determine the efficacy of viral-mediated recombination, we infected HEK293 cells with AAV-EGFP/Red and either AAV-Cre or AAV-CreER^{T2} (Fig. 1B). Co-infection of AAV-Cre and AAV-EGFP/Red resulted in expression of DsRed-Express-DR, while only d2EGFP was expressed in control cells infected with AAV-EGFP/Red alone. Co-infection with the reporter vector and AAV-CreER^{T2} induced DsRed-Express-DR expression in almost all 4-hydroxytamoxifen (4-OHT)-treated cells. Although we detected slight background expression of DsRed-Express-DR in the absence of 4-OHT, we observed only a limited number of these cells (<1%), indicating that CreER^{T2} activity is tightly regulated in these virally transduced cells. To test the potential use of AAV-CreER^{T2} *in vivo*, we used stereotaxic injections to deliver AAV-CreER^{T2} into the brains of reporter mice [10]. These mice were engineered to express a red-shifted variant of the wild-type green fluorescent protein (EGFP) only after Cre-mediated excision of a loxP DNA fragment. After 5 consecutive days of 4-OHT treatment (1 mg by intraperitoneal injection), we observed numerous EGFP-expressing cells in AAV-injected brains, all of which coexpressed Cre recombinase (Fig. 1C). In the absence of treatment with 4-OHT, only a few cells (<0.1% of Cre-positive cells) expressed EGFP in the vicinity of AAV-CreER^{T2}-injected sites (data not shown). These data indicate that floxed DNA segments are efficiently excised *in vivo* by combining AAV-CreER^{T2} injection with 4-OHT treatment.

Temporally Controlled Reduction of Dopamine Synthesis

We generated AAV vectors expressing each of the three dopamine-synthesizing enzymes (TH, AADC, and GCH). In the TH-expressing vector, two loxP sites flanked the TH coding sequence (AAV-floxed TH). We infected HEK293 cells with these dopamine-synthesizing vectors (AAV-floxed TH, AAV-AADC, and AAV-GCH) in combination

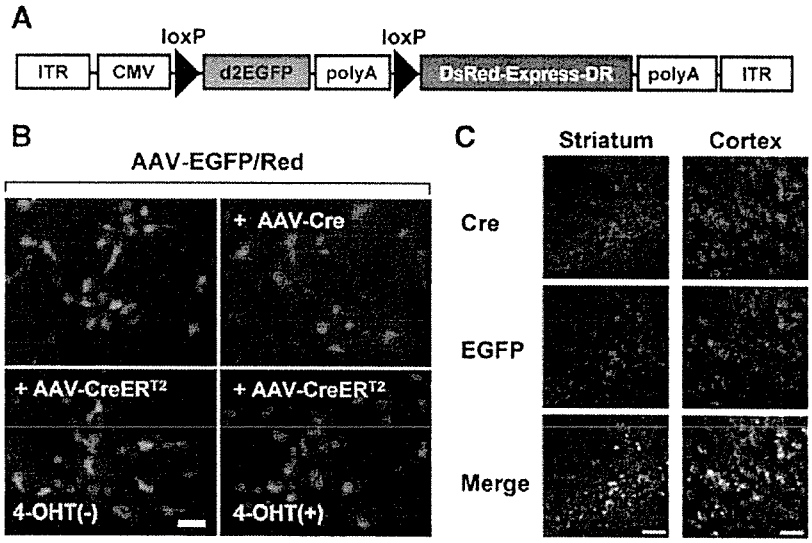

FIG. 1. Viral vector-mediated Cre-dependent floxed DNA excision. (A) Illustration of the AAV-EGFP/Red vector construct. A DsRed-Express-DR marker was placed downstream of the d2EGFP marker with a SV40 poly(A) sequence flanked by loxP sites. ITR, inverted terminal repeat; CMV, human cytomegalovirus immediate-early promoter followed by the first intron of human growth hormone. (B) 4-OHT-induced Cre-dependent recombination. HEK293 cells were infected with AAV-EGFP/Red and either AAV-Cre or AAV-CreER^{T2}. 4-OHT was added to the medium 5 h after infection. Fluorescence was observed 48 h after infection. Bar, 40 μm. (C) EGFP expression in the AAV-CreER^{T2}-injected striatum and cortex of transgenic mice. 4-OHT (1 mg) was administered intraperitoneally 1 week after vector injection every day for 5 days until the mice were killed. In these mice, the stop fragment was flanked by loxP sites and placed between the EGFP sequence and the *Gt(ROSA)26Sor* promoter. Bar, 40 μm.

doi:10.1016/j.ymthe.2005.08.009

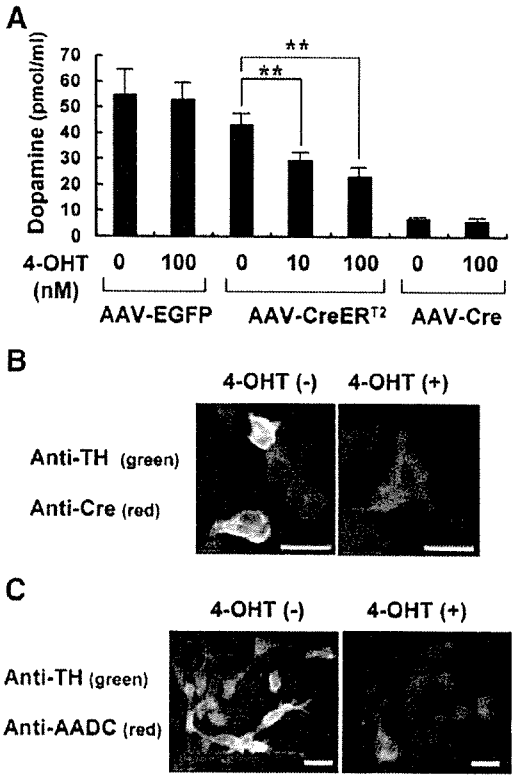

FIG. 2. Reduced dopamine synthesis after 4-OHT-induced ablation of a floxed TH transgene. HEK293 cells were infected with dopamine-synthesizing vectors (AAV-floxed TH, AAV-AADC, and AAV-GCH) in combination with AAV-CreER^{T2} or control vectors. (A) Dopamine content in the culture medium was significantly reduced in the presence of 4-OHT. $^{**}P < 0.01$, $n = 4$. (B) TH (green) and CreER^{T2} (red) immunocytochemistry was performed 48 h after vector infection. Yellow fluorescence in the merged image indicates colocalization. In the presence of 4-OHT, CreER^{T2} translocated to the nucleus. TH was not expressed in cells positive for nuclear CreER^{T2}. Bar, 20 μm. (C) TH (green) and AADC (red) immunocytochemistry. Note the reduced number of TH-positive cells in the presence of 4-OHT. Bar, 20 μm.

with AAV-CreER^{T2} or control vectors. We found that treatment with 4-OHT significantly reduced dopamine synthesis (Fig. 2A). Immunocytochemistry demonstrated coexpression of TH and CreER^{T2} in the cytoplasm in the absence of 4-OHT and an absence of TH expression when CreER^{T2} was translocated into the nucleus in the presence of 4-OHT (Fig. 2B). The expression of AADC was not reduced by the presence of 4-OHT (Fig. 2C). Dual labeling showed that more than 80% of the TH-immunoreactive (TH-IR) cells were also positive for AADC (251 of 300) and Cre (242 of 300) in the absence of 4-OHT-treatment.

Reduction of Dopamine Production in a Rat Model

We next tested whether the vector-mediated Cre-dependent regulation of transgene expression observed in culture could be extended to animal models. We obtained hemiparkinsonian rats by injecting a selective neurotoxin, 6-hydroxydopamine (6-OHDA), into the left medial forebrain bundle. The animals then received a mixture of AAV-CreER^{T2}, AAV-floxed TH, AAV-AADC, and AAV-GCH into their lesioned striatum, after which two-thirds were further treated with 4-OHT (4 mg/kg by intraperitoneal injection for 5 days) during the course of experimentation. Control rats were injected with AAV-LacZ alone or with AAV-Cre plus AAV-floxed TH, AAV-AADC, and AAV-GCH. To evaluate abnormal motor functions associated with depletion of dopamine in the striatum, we repeated quantification of apomorphine-induced rotation, as well

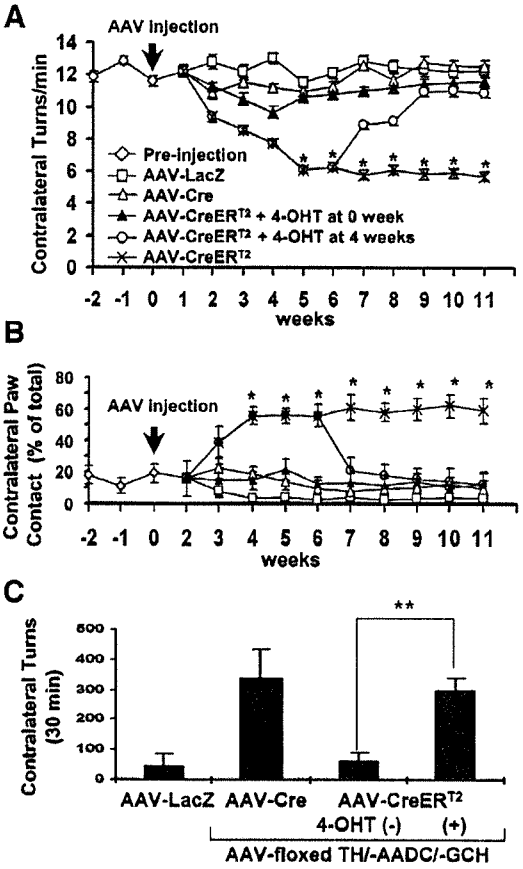

FIG. 3. Temporal control of dopamine synthesis in a rat model of PD transduced with AAV vectors. Sixty hemiparkinsonian rats were generated by 6-OHDA injection. Thirty-six received a mixture of AAV-CreER^{T2}, AAV-floxed TH, AAV-AADC, and AAV-GCH, after which they were divided into three groups of 12. Two of the groups were treated with 4-OHT (4 mg/kg by intraperitoneal injection for 5 days), at the same time or 4 weeks after vector injection. Control PD rats were injected with AAV-LacZ alone ($n = 12$) or AAV-Cre ($n = 12$), instead of AAV-CreER^{T2} with AAV-floxed TH, AAV-AADC, and AAV-GCH. (A) The total number of complete body turns induced by apomorphine was counted for each rat, and (B) spontaneous limb use was scored using the cylinder test. $^{*}P < 0.05$. (C) Efficient conversion of L-dopa to dopamine by AADC. L-Dopa (5 mg/kg) was administered to 4-OHT-treated rats and AAV-Cre-injected rats. Contralateral turning in response to L-dopa was counted for 30 min. $^{**}P < 0.01$. Legend symbols are as shown in A and B.

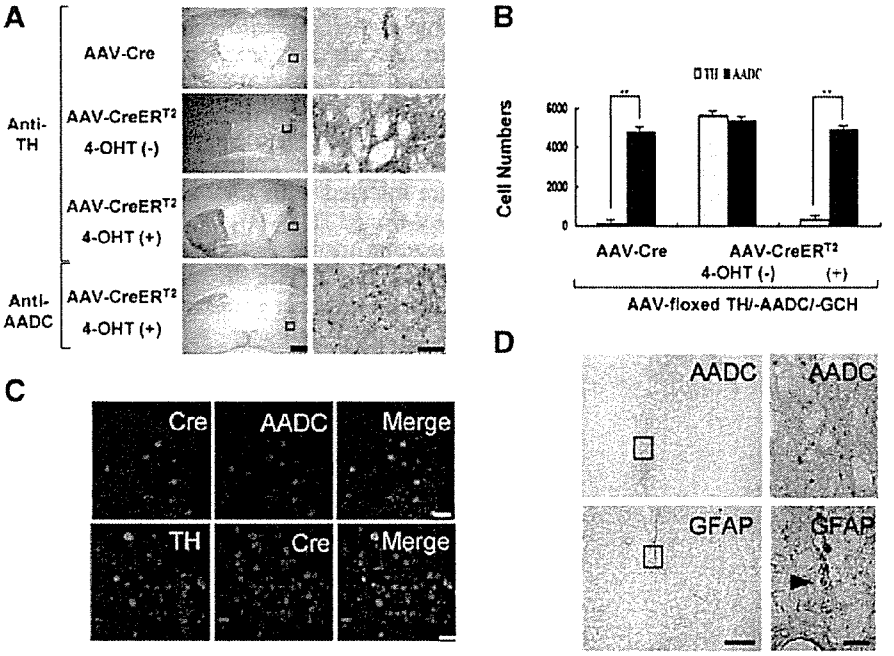

FIG. 4. Selective ablation of the TH transgene induced by treatment with 4-OHT. (A) Immunohistochemical staining for TH or AADC in the brains of 6-OHDA-lesioned rats 12 weeks after stereotaxic injection of AAV-Cre or AAV-CreER^{T2}, with or without 4-OHT treatment. AAV vectors were injected into the lesioned side of the striatum (right side of the photos). High-power-magnified images of the vector injection sites (squares in the left column) are shown in the right column. Representative photographs are also shown. Bar, 1.5 mm (left column), 100 μm (right column). (B) Number of immunoreactive (IR) cells against TH or AADC in the multiple AAV vector-injected striatum. The number of cells in 11 sections per rat (n = 3 for each group) was counted. The numbers of TH-IR cells and AADC-IR cells in AAV-CreER^{T2}-injected rats given 4-OHT 0 or 4 weeks after vector injection were indistinguishable and the results pooled for comparison with other groups. $^{**}P < 0.01$. (C) Efficient cotransduction of AAV vectors, as determined by dual immunofluorescence staining of the 6-OHDA-lesioned striatum. The majority of Cre-IR cells were also positive for TH and AADC. Bar, 20 μm. (D) Parallel striatal sections immunostained for glial fibrillary acidic protein (GFAP) or AADC. Striatal cells were transduced without obvious reactive astrocytosis. Residual hemosiderin was observed along the needle tract. On the right are magnified views of the boxes on the left. Bars: 0.5 mm, left; 50 μm, right.

as the cylinder test, weekly until the rats were killed. In the absence of 4-OHT, we observed behavioral recovery in rats that received both AAV-CreER^{T2} and AAV vectors expressing dopamine-synthesizing enzymes. Following 4-OHT treatment, these rats regressed, demonstrating impaired behavior (Figs. 3A and 3B). No recovery occurred in AAV-CreER^{T2}-injected rats treated with 4-OHT at the same time as vector injection or in AAV-Cre- or AAV-LacZ-injected rats. Contralateral turning in response to L-3,4-dihydroxyphenylalanine (L-dopa, 5 mg/kg) was not significantly reduced in 4-OHT-treated rats or AAV-Cre injected rats, indicating efficient conversion of L-dopa to dopamine in the striatum due to preservation of AADC activity (Fig. 3C).

Immunohistochemistry showed fewer TH-IR cells in rats that received AAV-Cre or AAV-CreER^{T2} plus 4-OHT, compared to injected rats not treated with 4-OHT (Figs. 4A and 4B). The numbers of AADC-immunoreactive cells,

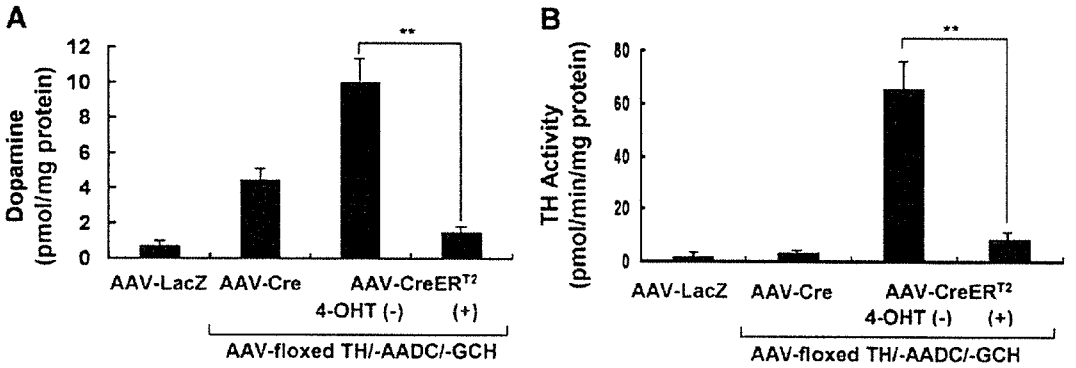

FIG. 5. Reduction of dopamine synthesis in 4-OHT-treated rats. Significantly less (A) dopamine content and (B) TH activity were observed in the lesioned striatum of 4-OHT-treated rats 12 weeks after vector injection, compared to 4-OHT-untreated rats. $^{**}P < 0.01$, n = 4.

doi:10.1016/j.ymthe.2005.08.009

however, did not differ significantly between 4-OHT-treated and untreated rats. We roughly estimated the number of transduced cells in the striatum at 5×10^4 based on cell counts performed on the tissue sections. This efficiency of transduction is sufficient to parallel the functional effects on behavior observed in other studies [3,5,11]. Double-labeling with both anti-Cre and anti-TH antibodies, or with anti-Cre and anti-AADC antibodies, showed that more than 80% of Cre-immunoreactive cells were also positive for TH (164 of 200) and AADC (176 of 200) in three 4-OHT-untreated rats (Fig. 4C). Immunostaining for glial fibrillary acidic protein (GFAP) or AADC in parallel sections demonstrated transduction of striatal cells without obvious reactive astrocytosis (Fig. 4D). Dopamine content (Fig. 5A) and TH activity (Fig. 5B) within the lesioned striatum were significantly lower in 4-OHT-treated compared to untreated rats. Dopamine levels in the transduced striatum in the 4-OHT-treated and untreated rats were 0.66 and 4.3%, respectively, those of the unlesioned striatum. Unlike primary dopamine in the nigrostriatal system, which is stored in synaptic vesicles, genetically produced dopamine in the lesioned striatum might be readily metabolized without storage. Since the dopamine level in the lesioned side of AAV-LacZ-injected rats was much lower (0.3%), a 10-fold increase in dopamine level after triple transduction with TH, AADC, and GCH genes caused a remarkable therapeutic effect. Average TH activity, measured in terms of L-dopa production (pmol/min/mg protein), reached 51.6% that of the normal striatum (65.9 ± 11.0 versus 127.7 ± 3.7) in rats transduced with dopamine-synthesizing enzymes. In 4-OHT-treated rats, TH activity fell to 10.8% of normal (13.8 ± 4.1).

Discussion

Our results show efficient viral vector-mediated delivery of tamoxifen-dependent $CreER^{T2}$ recombinase into rodent brains and that transgenic floxed sequences can be deleted in a temporally controlled manner. In a rat model of PD, recombinant AAV vector-mediated delivery of $CreER^{T2}$ into the striatum enabled 4-OHT-induced excision of a floxed TH transgene, resulting in reduced virally mediated dopamine synthesis. We targeted TH, a rate-limiting enzyme for dopamine biosynthesis that converts dietary L-tyrosine to L-dopa. Using this strategy, AADC activity was retained so that L-dopa, a substrate for AADC capable of crossing the blood–brain barrier, could be converted to dopamine in the striatum. Thus, in clinical situations, the therapeutic effects of orally administered L-dopa would likely be preserved, even after 4-OHT treatment to reduce TH expression in cases of dopamine overproduction [11]. Although transduction with AADC alone, in combination with oral administration of L-dopa, might not achieve continuous delivery of L-dopa, in contrast to that which could potentially be achieved with triple transduction of TH, AADC, and GCH, dopamine production could be regulated by altering the dose of L-dopa, thereby providing a safer option for gene therapy. We previously demonstrated that dopamine synthesis was enhanced (greater than fivefold) after systemic administration of L-dopa in AAV-TH/-AADC/-GCH-injected striatum in the primate model of PD using *in vivo* dialysis [4]. A phase I clinical trial involving gene transfer of AADC alone is currently under way.

AAV vectors are powerful tools by which to deliver therapeutic genes into the mammalian brain. Many striatal neurons of rodents and nonhuman primates are transduced with AAV vectors via stereotaxic injection, and long-term gene expression has been achieved without substantial toxicity or immune response [2,12]. AAV vectors have safety advantages over other viral vectors when it comes to *in vivo* gene delivery, since they are derived from nonpathogenic wild-type viruses. Moreover, most recombinant AAVs are present in cells as episomes, thus reducing the probability of insertional activation of oncogenes, compared to retroviruses, which integrate into host chromosomes [13]. Although it is difficult to use a single AAV vector for multiple gene transfer due to its limited packaging capacity (<5 kb), a single cell can be simultaneously transduced with multiple AAV vectors. In the present study, dual immunofluorescence staining showed efficient cotransduction of cells with different AAV vectors in the rat striatum, a finding consistent with that which we observed in a previous study [5].

Gene therapy strategies for the treatment of PD using AAV vectors include gene delivery of dopamine-synthesizing enzymes into the striatum to restore dopamine production, as well as gene delivery of neuroprotective molecules, such as glial cell line-derived neurotrophic factor, to block or slow down further degeneration [14]. In addition, AAV vectors harboring genes encoding neurotrophic factors might be delivered by intramuscular administration in an attempt to protect spinal motoneurons in patients suffering from amyotrophic lateral sclerosis [15–17]. Although no adverse effects due to overexpression of transgenes have been reported in animals to date, it is necessary to develop vectors that allow for regulation of transgene expression, thus avoiding transgene overexpression. In PD, overproduction of dopamine has the potential to cause dyskinesia or hallucinations, and sustained exposure to high concentrations of neurotrophic factors could result in tumor formation.

Inducible Cre recombinases have been used to generate a number of conditional knockout mice. They are invaluable tools for investigators studying the role of gene function in development, as well as a number of physiological and pathological processes. The tamoxifen-dependent $CreER^{T2}$ recombinase has proven particularly helpful [9,18,19]. It has been shown that 4-OHT does not alter dopamine content within the striatum in mice [20],

and we did not observe any adverse effects of 4-OHT treatment in the present experiment. In addition, tamoxifen, which is metabolized by the liver into 4-OHT, has neuroprotective effects [21,22]. Thus, the CreER^{T2} system might be useful for gene therapy in the treatment of neurological diseases.

We have expanded upon the use of inducible Cre recombinase technology to regulate transgene expression using an AAV vector-mediated gene delivery system. Recently, a viral vector-mediated RNA interference (RNAi) approach has been developed and localized gene knockdown achieved in the adult brain [23–25]. Although RNAi-mediated suppression of gene function has a wide variety of applications, more specific and inducible transgene silencing can be achieved with AAV-CreER^{T2}. Selective ablation of floxed transgenes reduces the possibility of down-regulation of normal cellular proteins. This system works as a molecular switch, increasing the safety of long-acting gene therapy by avoiding or minimizing side effects due to overproduction of the protein product and by providing the ability to shut down expression if toxicities are encountered or treatment is completed. The ability to restrict somatic recombination of transgenes spatially and temporally has a wide range of applications, in both gene therapy and biological study requiring somatic genetic manipulation.

Materials and Methods

AAV vector production. The AAV vector plasmids contained an expression cassette with a human cytomegalovirus immediate-early promoter (CMV promoter), followed by the first intron of human growth hormone, target cDNA, and a simian virus 40 polyadenylation signal sequence (SV40 poly(A)), between the inverted terminal repeats of the AAV-2 genome. The plasmids pAAV-LacZ, pEGFP, pAAV-AADC, pAAV-GCH, pCre, and pCreER^{T2} contained the cDNAs of LacZ, EGFP, human AADC, human GCH, Cre recombinase with a nuclear localization signal [26], and Cre recombinase fused to a mutated form of the ligand-binding domain of estrogen receptor α (CreER^{T2})[27], respectively. The plasmid pAAV-floxed TH contained human TH1 cDNA flanked by two loxP sequences between the CMV promoter and the SV40 poly(A). To generate pAAV-EGFP/Red, a DNA fragment containing d2EGFP (BD Biosciences, San Jose, CA, USA) and the SV40 poly(A) was flanked by loxP sequences and inserted between the CMV promoter and DsRed-Express-DR (BD Biosciences). The two helper plasmids, pHLP19 and pladenol (Avigen, Alameda, CA, USA), harbored the AAV *rep* and *cap* genes, as well as the *E2A*, *E4*, and *VA RNA* genes of the adenovirus genome, respectively. HEK293 cells were cotransfected by the calcium phosphate coprecipitation method with the vector plasmid, pHLP19, and pladenol. The AAV vectors were then harvested and purified by two rounds of continuous iodoxale ultracentrifugations. Vector titers were determined by quantitative DNA dot-blot hybridization or by quantitative PCR of DNase I-treated vector stocks. We routinely obtained 10^{12} to 10^{13} vector genome copies (vg).

In vitro transduction. HEK293 cells were seeded at 3×10^5 cells/well in six-well plates. After 24 h, cells were infected with appropriate combinations of AAV vectors (5×10^9 vg per vector). 4-OHT was added to the culture medium at a concentration of 10 or 100 nM at 5 h after infection. Culture medium was collected for dopamine assay 48 h after infection and the cells were fixed for immunostaining.

AAV injections. All animal experiments were performed in accordance with the institutional guidelines. Three B6,129-*Gt(ROSA))26Sor*^{tm2Sho}/J mice (The Jackson Laboratory, Bar Harbor, ME, USA) [10] were stereotaxically injected into the caudoputaminal unit or cerebral cortex with 1×10^9 vg (1 μl) of AAV-CreER^{T2}. After 1 week, 4-OHT (1 mg) was administered intraperitoneally every day for 5 days, after which 2 of the mice were killed. One mouse that did not receive 4-OHT treatment was killed as a control. Creation of PD model rats and stereotaxic injections of AAV vectors were carried out as previously described [5]. Briefly, 60 male albino Wistar rats (weighing 200–250 g) were unilaterally lesioned at the left medial forebrain bundle (coordinates AP −4.3 mm and ML 1.6 mm, relative to the bregma, and DV −7.8 mm relative to the dura, with the incisor bar set 3.3 mm below the interaural line) with 4 μl of 4.5 mg/ml 6-OHDA HBr (Sigma, St. Louis, MO, USA) in 0.02% ascorbate saline prior to intrastriatal transduction. These rats were stereotaxically injected with AAV vectors (5×10^7 vg per site for each vector) at three sites in the lesioned striatum (coordinates relative to the bregma and dura, AP +1.5, +1.0, and +0.5 mm; ML 2.6, 3.0, and 3.2 mm; DV −5.2 mm). Forty-eight rats were injected with a 1:1:1 mixture of AAV-floxed TH, AAV-AADC, and AAV-GCH plus AAV-Cre (n = 12) or AAV-CreER^{T2} (n = 36). Twelve rats received AAV-LacZ alone as a control. Among the AAV-CreER^{T2}-treated rats, 24 were intraperitoneally injected with 4-OHT (4 mg/kg) for 5 consecutive days, starting either at the same time as or 4 weeks after vector injection.

Behavioral testing. The rats were tested weekly for rotational behavior and spontaneous limb use, as described previously [28]. The total number of complete body turns was counted during an observation period of ≥ 60 min following intraperitoneal injection of apomorphine HCl (0.1 mg/kg; Sigma). Only those animals exhibiting seven or more contralateral rotations/min in a 60-min period at 4 weeks after the 6-OHDA injection were included in further analysis. Spontaneous limb use was scored according to the cylinder test method [29]. Rats were placed in a clear glass cylinder large enough to ensure free movement. After they had performed 10 rears during which they were observed to place at least one paw on the cylinder wall, the number of times both forepaws contacted the wall of the cylinder was counted until at least 20 contacts were made. Data indicating the number of times a contralateral forepaw made contact with the wall are expressed as a percentage of the total. We also evaluated rotational behavior in response to a low dose of L-dopa methyl ester (5 mg/kg; Sigma) coadministered with 2.5 mg/kg of a peripheral decarboxylase inhibitor (benserazide hydrochloride; Sigma) 10 weeks after AAV injection.

Biochemical assays. Levels of dopamine in the cell culture medium (n=4 for each group) and within the brain samples (n=4 for each group) were determined by high-performance liquid chromatography (HPLC), as previously described [5]. Rats were killed by decapitation under sodium pentobarbital anesthesia 12 weeks after vector injection, after which their brains were immediately dissected and placed on dry ice. The striatum was punched out bilaterally using a sharp-edged, stainless steel tube. Wet tissue samples were weighed and stored at −80°C until subsequent analysis. Tissues were homogenized in 20 volumes of homogenization buffer and then mixed immediately with 0.76 M perchloric acid prior to centrifugation at 15,000g for 10 min. After the supernatant was neutralized with sodium acetate, the samples were analyzed by HPLC analysis. Determination of TH activity was based on the formation of L-dopa from L-tyrosine, as demonstrated by HPLC electrochemical detection. The reaction mixture contained 200 mM sodium acetate buffer (pH 6.0), 100 mM 2-mercaptoethanol, 0.2 mg/ml catalase, 0.2 mM L-tyrosine, and 1 mM tetrahydrobiopterin. The mixture was incubated for 10 min at 37°C. The reaction was stopped by adding perchloric acid, and L-dopa was extracted using an alumina column [30].

Immunostaining of cultured cells and brain sections. Cultured cells were fixed in 4% paraformaldehyde (PFA) in PBS. Brains were perfused with 4% PFA, soaked in 30% sucrose, and dissected into coronal sections (30 μm). The following primary antibodies were used: TH monoclonal (1:800 or 1:8000; DiaSorin, Stillwater, MN, USA) or polyclonal (1:10,000; provided by Ikuko Nagatsu, Fujita Health University, Japan), AADC polyclonal (1:10,000; I. Nagatsu), Cre recombinase monoclonal (1:500; Covance, Princeton, NJ, USA) or polyclonal (1:500; Covance), GFP polyclonal (1:200; BD Biosciences or Chemicon, Temecula, CA, USA), DsRed

doi:10.1016/j.ymthe.2005.08.009

polyclonal (1:1000; BD Biosciences), and GFAP (1:1000; Chemicon). Appropriate fluorescence-tagged (Invitrogen, Carlsbad, CA, USA) or biotinylated (Vector Laboratories, Burlingame, CA, USA) secondary antibodies were used for visualization. Immunoreactivity was assessed under microscopy (Axioplan, Zeiss, Germany) or confocal laser scanning microscopy (TCS NT; Leica Microsystems, Germany). To analyze quantitatively the numbers of TH-positive neurons and AADC-positive neurons, every 10th 30-μm section (total of 11 sections) covering a 3-mm thickness from each animal ($n = 3$ per group) was examined. Coexpression efficacy was analyzed by dual immunofluorescence staining.

Statistical analysis. One-way analysis of variance (ANOVA) was performed to determine differences in dopamine levels, as well as TH activity, followed by Tukey's test (StatView 5.0 software; Abacus). Behavioral changes were analyzed by a repeated measure ANOVA, followed by Tukey's test, with $P < 0.05$ considered statistically significant. Results are presented as means ± SEM.

ACKNOWLEDGMENTS

We thank Avigen, Inc., for providing the AAV vector production system. This work was supported by grants from the Ministry of Education, Science, Sports, and Culture, as well as by funds made available by the Japanese Government for a High-Tech Research Center Project for Private Universities (2003–2005) and a University–Industry Joint Research Project (2003–2005). In addition, we received grants from the Japan Ministry of Health, Labor, and Welfare; a grant from The Ministere de l'Education Nationale, de l'Enseignement Superieur et de la Recherche; and funds from The Cell Science Research Foundation, the Centre National de la Recherche Scientifique, the Institut National de la Santé et de la Recherche Médicale, and the Collège de France.

RECEIVED FOR PUBLICATION MAY 14, 2005; REVISED JULY 26, 2005; ACCEPTED AUGUST 1, 2005.

REFERENCES

1. Burton, E. A., Glorioso, J. C., and Fink, D. J. (2003). Gene therapy progress and prospects: Parkinson's disease. *Gene Ther.* **10:** 1721–1727.
2. Muramatsu, S., *et al.* (2003). Adeno-associated viral vectors for Parkinson's disease. *Int. Rev. Neurobiol.* **55:** 205–222.
3. Mandel, R. J., *et al.* (1998). Characterization of intrastriatal recombinant adeno-associated virus-mediated gene transfer of human tyrosine hydroxylase and human GTP-cyclohydrolase I in a rat model of Parkinson's disease. *J. Neurosci.* **18:** 4271–4284.
4. Muramatsu, S., *et al.* (2002). Behavioral recovery in a primate model of Parkinson's disease by triple transduction of striatal cells with adeno-associated viral vectors expressing dopamine-synthesizing enzymes. *Hum. Gene Ther.* **13:** 345–354.
5. Shen, Y., *et al.* (2000). Triple transduction with adeno-associated virus vectors expressing tyrosine hydroxylase, aromatic-L-amino-acid decarboxylase, and GTP cyclohydrolase I for gene therapy of Parkinson's disease. *Hum. Gene Ther.* **11:** 1509–1519.
6. Rajewsky, K., *et al.* (1996). Conditional gene targeting. *J. Clin. Invest.* **98:** 600–603.
7. Branda, C. S., and Dymecki, S. M. (2004). Talking about a revolution: the impact of site-specific recombinases on genetic analyses in mice. *Dev. Cell* **6:** 7–28.
8. Metzger, D., and Feil, R. (1999). Engineering the mouse genome by site-specific recombination. *Curr. Opin. Biotechnol.* **10:** 470–476.
9. Metzger, D., *et al.* (2003). Targeted conditional somatic mutagenesis in the mouse: temporally-controlled knock out of retinoid receptors in epidermal keratinocytes. *Methods Enzymol.* **364:** 379–408.
10. Mao, X., *et al.* (2001). Activation of EGFP expression by Cre-mediated excision in a new ROSA26 reporter mouse strain. *Blood* **97:** 324–326.
11. Sanchez-Pernaute, R., Harvey-White, J., Cunningham, J., and Bankiewicz, K. S. (2001). Functional effect of adeno-associated virus mediated gene transfer of aromatic L-amino acid decarboxylase into the striatum of 6-OHDA-lesioned rats. *Mol. Ther.* **4:** 324–330.
12. Tenenbaum, L., *et al.* (2004). Recombinant AAV-mediated gene delivery to the central nervous system. *J. Gene Med.* **6**(Suppl. 1)**:** S212–S222.
13. McCarty, D. M., Young, S. M., Jr., and Samulski, R. J. (2004). Integration of adeno-associated virus (AAV) and recombinant AAV vectors. *Annu. Rev. Genet.* **38:** 819–845.
14. Hurelbrink, C. B., and Barker, R. A. (2004). The potential of GDNF as a treatment for Parkinson's disease. *Exp. Neurol.* **185:** 1–6.
15. Azzouz, M., *et al.* (2004). VEGF delivery with retrogradely transported lentivector prolongs survival in a mouse ALS model. *Nature* **429:** 413–417.
16. Kaspar, B. K., *et al.* (2003). Retrograde viral delivery of IGF-1 prolongs survival in a mouse ALS model. *Science* **301:** 839–842.
17. Wang, L. J., *et al.* (2002). Neuroprotective effects of glial cell line-derived neurotrophic factor mediated by an adeno-associated virus vector in a transgenic animal model of amyotrophic lateral sclerosis. *J. Neurosci.* **22:** 6920–6928.
18. Imai, T., *et al.* (2004). Peroxisome proliferator-activated receptor gamma is required in mature white and brown adipocytes for their survival in the mouse. *Proc. Natl. Acad. Sci. USA* **101:** 4543–4547.
19. Simon, D., *et al.* (2004). Friedreich ataxia mouse models with progressive cerebellar and sensory ataxia reveal autophagic neurodegeneration in dorsal root ganglia. *J. Neurosci.* **24:** 1987–1995.
20. Kuo, Y. M., *et al.* (2003). 4-Hydroxytamoxifen attenuates methamphetamine-induced nigrostriatal dopaminergic toxicity in intact and gonadectomized mice. *J. Neurochem.* **87:** 1436–1443.
21. Ciriza, I., *et al.* (2004). Selective estrogen receptor modulators protect hippocampal neurons from kainic acid excitotoxicity: differences with the effect of estradiol. *J. Neurobiol.* **61:** 209–221.
22. Obata, T., and Kubota, S. (2001). Protective effect of tamoxifen on 1-methyl-4-phenylpyridine-induced hydroxyl radical generation in the rat striatum. *Neurosci. Lett.* **308:** 87–90.
23. Harper, S. Q., *et al.* (2005). RNA interference improves motor and neuropathological abnormalities in a Huntington's disease mouse model. *Proc. Natl. Acad. Sci. USA* **102:** 5820–5825.
24. Hommel, J. D., *et al.* (2003). Local gene knockdown in the brain using viral-mediated RNA interference. *Nat. Med.* **9:** 1539–1544.
25. Xia, H., *et al.* (2004). RNAi suppresses polyglutamine-induced neurodegeneration in a model of spinocerebellar ataxia. *Nat. Med.* **10:** 816–820.
26. Kalderon, D., Roberts, B. L., Richardson, W. D., and Smith, A. E. (1984). A short amino acid sequence able to specify nuclear location. *Cell* **39:** 499–509.
27. Feil, R., Wagner, J., Metzger, D., and Chambon, P. (1997). Regulation of Cre recombinase activity by mutated estrogen receptor ligand-binding domains. *Biochem. Biophys. Res. Commun.* **237:** 752–757.
28. Wang, L., *et al.* (2002). Delayed delivery of AAV-GDNF prevents nigral neurodegeneration and promotes functional recovery in a rat model of Parkinson's disease. *Gene Ther.* **9:** 381–389.
29. Schallert, T., *et al.* (2000). CNS plasticity and assessment of forelimb sensorimotor outcome in unilateral rat models of stroke, cortical ablation, parkinsonism and spinal cord injury. *Neuropharmacology* **39:** 777–787.
30. Nagatsu, T., Oka, K., and Kato, T. (1979). Highly sensitive assay for tyrosine hydroxylase activity by high-performance liquid chromatography. *J. Chromatogr.* **163:** 247–252.

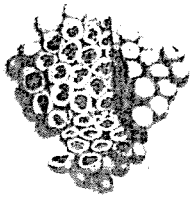

STEM CELLS®

Improved Safety of Hematopoietic Transplantation with Monkey Embryonic Stem Cells in the Allogeneic Setting

Hiroaki Shibata, Naohide Ageyama, Yujiro Tanaka, Yukiko Kishi, Kyoko Sasaki, Shinichiro Nakamura, Shin-ichi Muramatsu, Satoshi Hayashi, Yoshihiro Kitano, Keiji Terao and Yutaka Hanazono

Stem Cells 2006;24;1450-1457; originally published online Feb 2, 2006;
DOI: 10.1634/stemcells.2005-0391

STEM CELLS
EMBRYONIC STEM CELLS

Improved Safety of Hematopoietic Transplantation with Monkey Embryonic Stem Cells in the Allogeneic Setting

HIROAKI SHIBATA,[a,b] NAOHIDE AGEYAMA,[b] YUJIRO TANAKA,[a] YUKIKO KISHI,[a] KYOKO SASAKI,[a] SHINICHIRO NAKAMURA,[b,c] SHIN-ICHI MURAMATSU,[d] SATOSHI HAYASHI,[e] YOSHIHIRO KITANO,[f] KEIJI TERAO,[b] YUTAKA HANAZONO[a]

[a]Division of Regenerative Medicine, Center for Molecular Medicine, Jichi Medical University, Tochigi, Japan; [b]Tsukuba Primate Research Center, National Institute of Biomedical Innovation, Ibaraki, Japan; [c]Department of Veterinary Pathology, Nippon Veterinary and Animal Science University, Tokyo, Japan; [d]Department of Neurology, Jichi Medical University, Tochigi, Japan; Departments of [e]Obstetrics and Gynecology and [f]Surgery, National Center for Child Hearth and Development, Tokyo, Japan

Key Words. Cynomolgus monkey • Hematopoiesis • Embryonic stem cell • In utero transplantation • Teratoma • Purging Tumor prevention

ABSTRACT

Cynomolgus monkey embryonic stem cell (cyESC)-derived in vivo hematopoiesis was examined in an allogeneic transplantation model. cyESCs were induced to differentiate into the putative hematopoietic precursors in vitro, and the cells were transplanted into the fetal cynomolgus liver at approximately the end of the first trimester (n = 3). Although cyESC-derived hematopoietic colony-forming cells were detected in the newborns (4.1%–4.7%), a teratoma developed in all newborns. The risk of tumor formation was high in this allogeneic transplantation model, given that tumors were hardly observed in immunodeficient mice or fetal sheep that had been xeno-transplanted with the same cyESC derivatives. It turned out that the cyESC-derived donor cells included a residual undifferentiated fraction positive for stage-specific embryonic antigen (SSEA)-4 (38.2% ± 10.3%) despite the rigorous differentiation culture. When an SSEA-4-negative fraction was transplanted (n = 6), the teratoma was no longer observed, whereas the cyESC-derived hematopoietic engraftment was unperturbed (2.3%–5.0%). SSEA-4 is therefore a clinically relevant pluripotency marker of primate embryonic stem cells (ESCs). Purging pluripotent cells with this surface marker would be a promising method of producing clinical progenitor cell preparations using human ESCs. STEM CELLS *2006;24:1450–1457*

INTRODUCTION

Human embryonic stem cells (hESCs) hold great potential in the treatment of a variety of diseases and injuries because embryonic stem cells (ESCs) have the ability to proliferate indefinitely in culture and to differentiate into any cell type [1, 2]. Because ESCs are able to form teratomas when transplanted into immunodeficient mice, safety concerns would be raised against the clinical application of hESCs [3, 4]. It will be necessary to test the safety of these cells in animal transplantation models before clinical application. Nonhuman primate transplantation models would be desirable for this purpose; however, there have been only a few reports on these models [5–7]. The successful engraftment of transplanted cells in primates will not be achieved unless the immune rejection of transplanted cells is circumvented (e.g., through immunosuppressive treatment) [6]. The early gestational fetus may be a good recipient with which to circumvent immune rejection because the immune system is premature [8]. In addition, in the animal fetus, transplanted cells would engraft without conditioning of recipients such as irradiation or immunosuppressive treatment [9–12]. We have previously established a system for allogeneic transplantation of cynomolgus ESCs (cyESCs) using preimmune fetal monkeys as recipients [5].

We have also reported a novel method for hematopoietic engraftment from cyESCs in sheep [13]. The method is a combination of three steps: (a) differentiation in vitro to generate the putative hematopoietic precursors [14]; (b) transplantation of the cells in utero [15]; and (c) development into hematopoietic cells in vivo using the hematopoietic microenvironment of the fetal liver [16]. In the present study,

Correspondence: Yutaka Hanazono, M.D., Ph.D., Division of Regenerative Medicine, Center for Molecular Medicine, Jichi Medical University, 3311-1 Yakushiji, Shimotsuke, Tochigi 329-0498, Japan. Telephone: +81-285-58-7450; Fax: +81-285-44-5205; e-mail: hanazono@jichi.ac.jp Received on August 13, 2005; accepted for publication on January 23, 2006; first published online in STEM CELLS *EXPRESS* February 2, 2006. 1066-5099/2006/$20.00/0 doi: 10.1634/stemcells.2005-0391

we have examined the safety as well as the efficacy of hematopoietic engraftment of cells derived from cyESCs in the allogeneic transplantation model.

MATERIALS AND METHODS

Animals

Pregnant cynomolgus monkeys (16–22 years old) were obtained by mating and were reared at the Tsukuba Primate Research Center in accordance with Rules for Animals Care and Management set forth by the Research Center and Guiding Principles for Animal Experiments Using Nonhuman Primates formulated by the Primate Society of Japan. Experimental procedures were approved by the Animal Welfare and Animal Care Committee of the National Institute of Infectious Diseases. The animals were free of intestinal parasites and were seronegative for herpes virus B, varicella-zoster-like virus, measles virus, and simian immunodeficiency virus.

Cell Preparation

A cyESC line (CMK6G) stably expressing green fluorescent protein (GFP) was established after transfection of the parental cyESC line (CMK6) with the enhanced GFP gene (Clontech, Palo Alto, CA, http://www.clontech.com) [17]. cyESCs were maintained on a feeder layer of mitomycin C (Kyowa, Tokyo, http://www.kyowa.co.jp)-treated mouse (ICR or BALB/c; Clea Japan, Tokyo, http://www.clea-japan.com) embryonic fibroblasts as previously described [18]. The mouse bone marrow stromal cell line OP9 was maintained in α-minimum essential medium (Invitrogen, Carlsbad, CA, http://www.invitrogen.com) supplemented with 20% fetal calf serum (FCS; Invitrogen) [19].

cyESCs were induced to differentiate into the putative hematopoietic precursors as previously described [13]. Briefly, undifferentiated cyESCs were transferred onto mitomycin C-treated confluent OP9 cells and cultured for 6 days in Iscove's modified Dulbecco's medium (Invitrogen) supplemented with 8% FCS, 8% horse serum (Invitrogen), 5×10^{-6} M hydrocortisone (Sigma, St. Louis, http://www.sigmaaldrich.com), and multiple cytokines, including 20 ng/ml recombinant human (rh) bone morphogenetic protein-4 (R&D Systems, Minneapolis, http://www.rndsystems.com), 20 ng/ml rh stem cell factor (Biosource, Camarillo, CA, http://www.biosource.com), 20 ng/ml rh vascular endothelial growth factor (VEGF; R&D Systems), 20 ng/ml rh Flt-3 ligand (PeproTech, Rocky Hill, NJ, http://www.peprotech.com), 20 ng/ml rh interleukin-3 (PeproTech), 10 ng/ml rh interleukin-6 (PeproTech), 20 ng/ml rh granulocyte colony-stimulating factor (PeproTech), and 2 IU/ml rh erythropoietin (Roche, Basel, Switzerland, http://www.roche.com). The cells were resuspended in 0.1% human serum albumin (Sigma)/Hanks' balanced saline solution (Sigma) for transplantation.

Flow Cytometry

Primary antibodies (Abs) used in the present study were anti-human CD34 monoclonal Ab (mAb; BD Pharmingen, San Diego, http://www.bdbiosciences.com/pharmingen), anti-human CD31 mAb (Pharmingen), anti-human CD45 mAb (Pharmingen), anti-human vascular endothelial (VE) cadherin mAb (Pharmingen), rabbit anti-human VEGF receptor (VEGFR)-2 Ab (Santa Cruz Biotechnology, Santa Cruz, CA, http://www.scbt.com), and anti-stage-specific embryonic antigen (SSEA)-4 mAb (Chemicon, Temecula, CA, http://www.chemicon.com). All of them cross-reacted to cynomolgus counterparts as previously demonstrated [18, 20–22]. Secondary Abs were phycoerythrin (PE)-conjugated rabbit anti-mouse immunoglobulins (Ig) Ab (DakoCytomation, Glostrup, Denmark, http://www.dako.com) and Alexa Fluor 647-conjugated goat anti-mouse IgG Ab (Molecular Probes, Eugene, OR, http://probes.invitrogen.com). Cells stained with unlabeled primary Abs were incubated with fluorescence-labeled secondary Abs. Cells were incubated with either primary or secondary Ab for 20–60 minutes at 4°C. Regarding staining with the anti-VEGFR-2 Ab, the cells were incubated with biotin-conjugated goat anti-rabbit IgG Ab (Beckman Coulter, Miami, http://www.beckmancoulter.com), followed by PE-conjugated streptavidin (Beckman Coulter). Fluorescence-labeled cells were analyzed with a FACS Calibur flow cytometer (Becton, Dickinson and Company, Franklin Lakes, NJ, http://www.bd.com). Data analysis was performed using the CellQuest software (Becton, Dickinson and Company). Isotype-matched, irrelevant mAbs (DakoCytomation or Beckman Coulter) served as negative controls. Nonviable cells were excluded from analysis by propidium iodide (Sigma) costaining.

Cell Sorting

Cell sorting was performed to purge SSEA-4$^+$ cells from among the cultured cyESCs in vitro. Cells were incubated with the anti-SSEA-4 mAb for 1 hour at 4°C and washed twice with Dulbecco's modified Eagle's medium supplemented with 10% FCS. The cells were then incubated with the PE-conjugated anti-mouse Ig Ab for 1 hour at 4°C and washed twice again. GFP-positive and SSEA-4-negative cells were sorted using an Epics Elite cell sorter (Beckman Coulter). Data acquisition was performed using the Expo2 software (Beckman Coulter).

Transplantation and Delivery

Transplant procedures were previously described [5]. Briefly, animals were anesthetized via an intramuscular administration of ketamine hydrochloride (Ketalar, 10 mg/kg; Sankyo, Tokyo, http://www.sankyo.co.jp) and received 0.5%–1.0% isoflurane by inhalation by means of an endotracheal tube. Cells ($0.16–46 \times 10^6$ cells per fetus; Table 1) were injected into the fetal liver through a 23-gauge needle using an ultrasound-guided technique at approximately the end of the first trimester. The fetuses were delivered by cesarean section at 2–3 months after transplant (gestation 120–157 days, full term 165 days).

Colony Polymerase Chain Reaction

Cynomolgus clonogenic hematopoietic colonies were produced as previously described [20]. After cells were cultured in methylcellulose medium for 10–14 days, well-separated individual colonies were plucked into 50 μl of distilled water and digested with 20 μg/ml proteinase K (Takara, Shiga, Japan, http://www.takara-bio.com) at 55°C for 1 hour, followed by 99°C for 10 minutes. Each sample (5 μl) was used for a nested polymerase chain reaction (PCR) to detect the *GFP* gene sequence. The outer primer set was 5′-AAGGACGACGGCAACTACAA-3′ and 5′-ACTGGGTGCTCAGGTAGTGG-3′, and the inner primer set was 5′-GCATCGACTTCAAGGAGGAC-3′ and 5′-GTTGTGGCGGATCTTGAAGT-3′. Amplification conditions for both the outer and inner PCR were 30 cycles of 95°C for 30 seconds, 65°C for 30 seconds, and 72°C for 30 seconds. The

Table 1. ESC-derived hematopoiesis and tumor formation

Animals	Animal no.	Transplanted cells	Purging SSEA-4$^+$ cells	Cell number per fetus ($\times 10^6$)	Donor-derived CFU in recipients[a] at birth (donor/total colony number)	Tumor formation	Observation period (months)
Monkeys	0031	Undifferentiated	−	3.90	n.d.	+	3
	2311	ESCs	−	0.16	n.d., Dead	+	2
	0321		−	0.21	n.d., Dead	+	2
	0841	Day-6 ESC-	−	10	4.1% (2/49)	+	3
	1551	derived cells	−	46	n.d., Dead	+	2.5
	0021		−	46	4.7% (4/85)	+	3
	0691	Day-6 ESC-	+	0.16	3.2% (2/62)	−	3
	0381	derived cells	+	1.40	5.0% (4/80)	−	3
	0022		+	0.17	2.3% (2/86)	−	3
	0981		+	0.31	4.1% (3/73)	−	3
	0051		+	0.31	n.d., Dead[b]	−	3
	1552		+	0.75	4.4% (2/45)	−	4
Sheep[c]	57	Day-6 ESC-	−	50	1.1% (1/91)	−	18
	55	derived cells	−	50	1.1% (1/91)	−	26
	141		−	78	1.1% (1/91)	−	26
	182		−	14	1.6% (1/63)	−	21

[a]Percentage of donor-derived CFU was calculated by dividing the number of CFU positive for the green fluorescent protein gene sequence by the number of CFU positive for the β-actin gene sequence. Donor-derived CFU were analyzed at delivery.
[b]Death due to ablation of placentae. Other deaths were presumably tumor-related.
[c]As published by Sasaki et al. [13].
Abbreviations: CFU, colony-forming units; ESC, embryonic stem cell; n.d., not done; SSEA, stage-specific embryonic antigen.

outer PCR products were purified using a QIA quick PCR purification kit (Qiagen, Valencia, CA, http://www.qiagen.com). Simultaneous PCR for the β-actin sequence was also performed to ensure DNA amplification of the sample in each colony. The primer set for β-actin was 5′-CATTGTCATGGACTCTGGCGACGG-3′ and 5′-CATCTCCTGCTCGAAGTCTAGGGC-3′. Amplification conditions for β-actin PCR were 40 cycles of 95°C for 30 seconds, 65°C for 30 seconds, and 72°C for 30 seconds. Amplified GFP (131 bp) and β-actin (234 bp) products were resolved on 2% agarose gel (Sigma) and visualized by ethidium bromide (Invitrogen) staining.

RNA PCR

Total RNA was extracted from cells of interest using the EZ1 RNA universal tissue kit (Qiagen). RNA was reverse-transcribed at 50°C for 30 minutes using the RNA LA PCR kit (Takara) with oligo dT primer. The resulting cDNA was then subjected to PCR. Regarding PCR for Oct-4, the primer set was 5′-GGACACCTGGCTTCGGATT-3′ and 5′-TTCGCTTTCTCTTTCGGGC-3′. The PCR conditions were 35 cycles of 95°C for 30 seconds, 67°C for 45 seconds, and 68°C for 1.5 minutes. Regarding PCR for Scl, the primer set was 5′-GGGCGGAAAGCTGTTTGCGATT-3′ and 5′-TCGCTGAGAGGCCTGCAGTT-3′. The PCR conditions were 35 cycles of 95°C for 30 seconds, 63°C for 1 minute, and 72°C for 1 minute. A simultaneous PCR for β-actin was also conducted on each cDNA sample as an internal control as described above. Amplified Oct-4 (697 bp), Scl (201 bp), and β-actin (234 bp) products were resolved on 2% agarose gel and visualized by ethidium bromide staining.

RESULTS

In Utero Transplantation and Delivery

cyESCs stably expressing GFP were used in this study [17]. In the setting of allogeneic transplantation, GFP was used as a genetic tag to track transplanted cell progeny. We employed the OP9 stromal cell coculture method instead of the embryoid body formation method to facilitate the hematopoietic differentiation [19, 23, 24] (Fig. 1A, 1B). According to the flow cytometric analysis, CD34, CD31 (platelet/endothelial cell adhesion molecule-1 [PECAM-1]), CD144 (VE-cadherin), and VEGFR-2 (Flk-1) were all upregulated on day 6 but decreased thereafter (Fig. 1C–1E, 1G). Among the markers examined, CD34 is a widely used surface marker of hematopoietic stem cells in both human and monkey subjects [25–27]. The others are key markers of hemangioblasts (which generate endothelial and hematopoietic lineages) in both mice and humans [14, 28]. Cells positive for both VEGFR-2 and VE-cadherin emerged on day 6 (Fig. 1H). CD45, however, was not detected until day 12 (Fig. 1F). Despite the hemangioblast marker expression on day 6, the hematopoietic *Scl* gene was upregulated at this time point as assessed by RNA PCR (Fig. 1I), implying that the hematopoietic commitment might have already occurred on day 6 [29, 30]. We therefore designated the day 6 cyESC-derived progenitor cells as putative hematopoietic precursors. The time course profiles presented here were similar to those of hESCs [14, 24]. The GFP expression was stable during the 6-day culture (Fig. 1A, 1B) and afterward (data not shown).

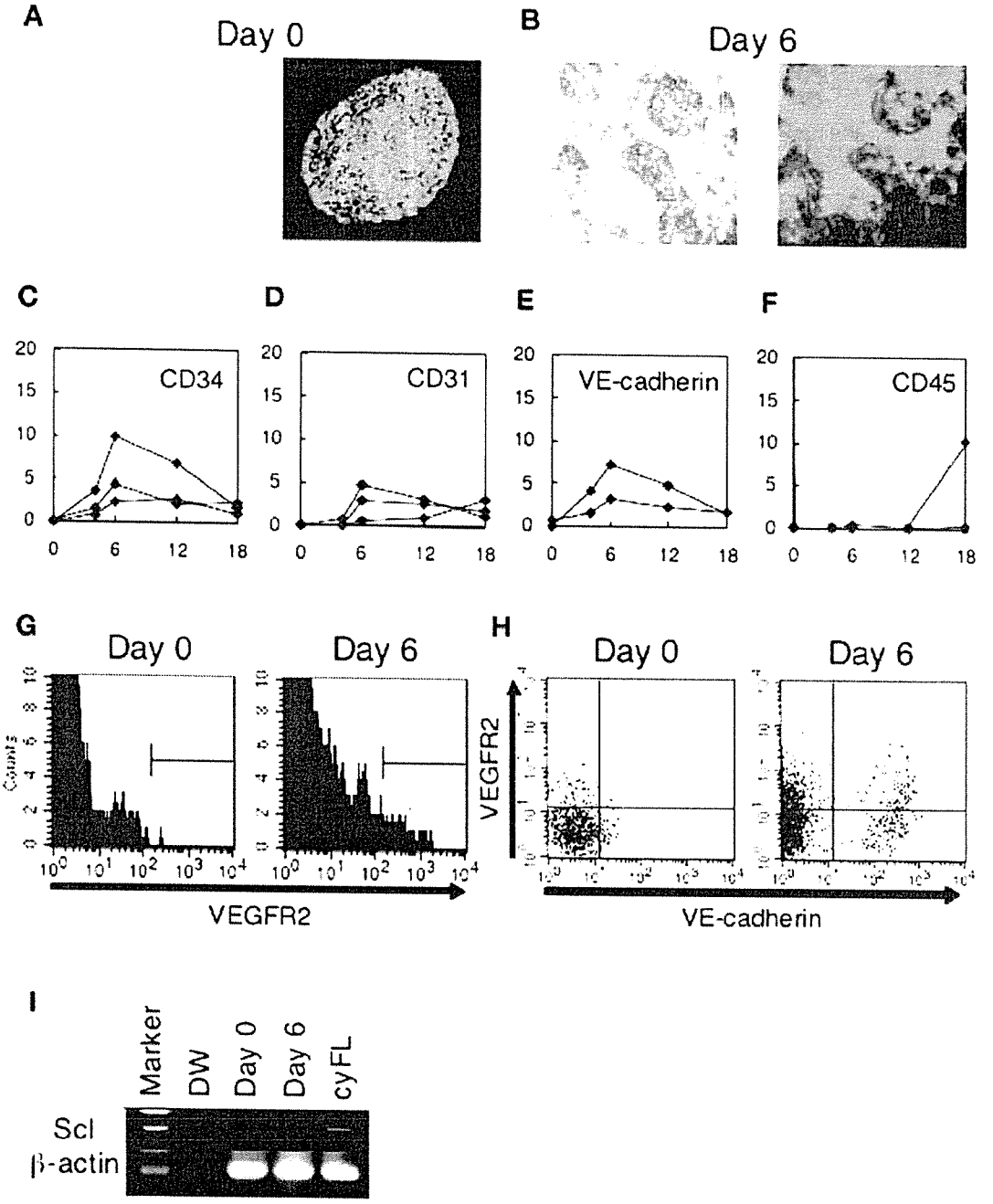

Figure 1. Flow cytometric analysis during the in vitro differentiation of cyESCs. Undifferentiated cyESCs expressing green fluorescent protein were cultured on OP9 cells with multiple cytokines (see Materials and Methods). **(A):** Cells on day 0 are shown in bright (left) and dark (right) fields. **(B):** Cells on day 6 are shown in bright (left) and dark (right) fields. **(C):** Cells on days 0, 4, 6, 12, and 18 were stained for CD34. **(D):** Cells on days 0, 4, 6, 12, and 18 were stained for CD31. **(E):** Cells on days 0, 4, 6, 12, and 18 were stained for VE-cadherin. **(F):** Cells on days 0, 4, 6, 12, and 18 were stained for CD45. The vertical axis shows the fraction (percentage) of cells that were stained positive. **(C–F):** Results of two or three independent experiments are shown. **(G):** Although cells on day 0 already express low levels of VEGFR-2, a VEGFR-2^{high} population did not emerge until day 6. **(H):** Dot-plot profiles for VEGFR-2 and VE-cadherin expression indicate that cells positive for both VEGFR-2 and VE-cadherin emerged until day 6. **(G, H):** Representative results from three independent experiments are shown. **(I):** The *Scl* gene expression was upregulated on day 6 to a level similar to that in the cynomolgus fetal liver as assessed by RNA polymerase chain reaction. Day-6 cells (putative hematopoietic precursors) were used for transplantation. Abbreviations: cyESC, cynomolgus embryonic stem cell; cyFL, cynomolgus fetal liver; DW, distilled water; VE, vascular endothelial; VEGFR, vascular endothelial growth factor receptor.

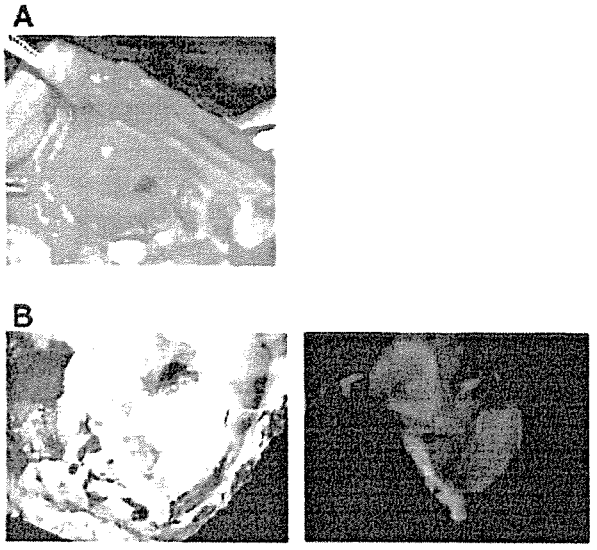

Figure 2. Tumor formation after the transplantation of cynomolgus embryonic stem cell (cyESC)-derived progenitor cells. Tumors formed in all three monkey fetuses transplanted with the day-6 cyESC-derived progenitor cells (putative hematopoietic precursors). (A): A representative tumor in the thoracic cavity at 3 months after transplantation (monkey no. 0841). (B): The tumor was observed in bright (left) and dark (right) fields under a fluorescence microscope.

Teratoma Formation

The undifferentiated cyESCs ($n = 3$) or cyESC-derived putative hematopoietic precursors ($n = 3$) were transplanted in utero into allogeneic fetuses in the liver under ultrasound guidance at approximately the end of the first trimester (49–66 days, full term 165 days) (Table 1). Regardless of whether the undifferentiated cyESCs or putative hematopoietic precursors were transplanted, tumors were found in the thoracic or abdominal cavities in all the six animals at 2–3 months after transplant (Table 1; Fig. 2A). The tumors fluoresced (Fig. 2B) and consisted of three germ layer cells. Thus, they were teratomas derived from transplanted cells. However, tumors were hardly observed in fetal sheep (1/10; [13] and our unpublished data) (Table 1) and immunodeficient (nonobese diabetic/severe combined immunodeficient) mice (3/10; our unpublished data) after the same putative hematopoietic precursors were transplanted.

In Vivo cyESC-Derived Hematopoiesis

Regarding the newborn monkeys that had been transplanted with the putative hematopoietic precursors, we harvested cells from the femur, cord blood, and liver and plated the cells in methylcellulose medium to produce clonogenic hematopoietic colonies (colony-forming units [CFU]) (Fig. 3A). The monkey cells generated colonies of clear hematopoietic morphology in this assay (Fig. 3B). To detect transplanted cell-derived, GFP-positive colonies, we tried to observe GFP fluorescence of colonies under a fluorescent microscope but were hampered by the high autofluorescence. We then conducted PCR for the *GFP* gene sequence in DNA isolated from each colony (colony PCR) (Fig. 3C). The transplanted cell-derived CFU were clearly detected in the animals (4.1% and 4.7%; Table 1). We repeated the colony PCR and confirmed that the results were reproducible.

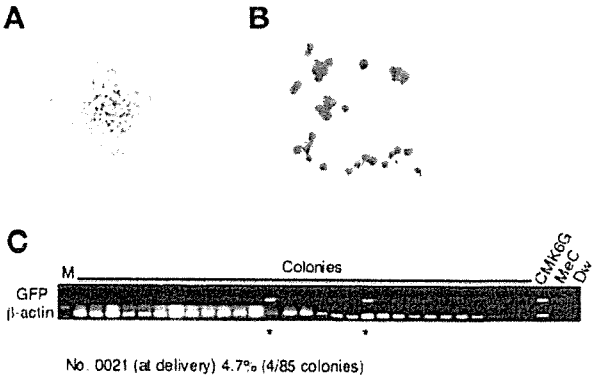

Figure 3. cyESC-derived hematopoiesis in vivo. (A): Bone marrow, cord blood, and liver cells were harvested from newborn monkeys and placed in methylcellulose medium to produce clonogenic hematopoietic colonies. (B): A cytospin specimen (stained with the May-Giemsa method) of plucked colonies reveals mature neutrophils. To identify cyESC-derived colonies, well-separated individual colonies were plucked and examined for the GFP sequence by PCR. Plucked MeC alone (not containing colonies) served as a negative control. PCR of the β-actin sequence in the same colonies was simultaneously performed as an internal control. Colony PCR was repeated at least twice. (C): Representative colony PCR results for monkey no. 0021. Asterisk indicates bands positive for the GFP sequence. Abbreviations: CMK6G, positive control green fluorescent protein-expressing cynomolgus cells; cyESC, cynomolgus embryonic stem cell; DW, distilled water; GFP, green fluorescent protein; M, molecular weight marker; MeC, methylcellulose; PCR, polymerase chain reaction.

We detected both granulocytic and erythroid cynomolgus CFU. In the peripheral blood, however, we were not able to detect cells expressing GFP by flow cytometry. It turned out that, as assessed by quantitative PCR, the fractions of GFP-positive cells in the peripheral blood were very small (<0.1%). Low peripheral "chimerism" has been reported more than once in other in utero transplantations of ESCs or hematopoietic stem cells such as in mice, sheep, and pigs [13, 31–33].

Purging SSEA-4$^+$ Cells of the Putative Hematopoietic Precursors

We examined the expression of an undifferentiated primate ESC marker, SSEA-4, in the undifferentiated cyESCs (day 0) and putative hematopoietic precursors (day 6). The proportion of SSEA-4$^+$ cells was 93.4% ± 8.1% and 38.2% ± 10.3% among the day-0 and -6 cells, respectively (Fig. 4A). A substantial number of cells were still positive for SSEA-4 after the rigorous differentiation culture. In addition, a considerable number of cells expressing another undifferentiated marker, Oct-4, remained among the day-6 population as assessed by RNA-PCR (Fig. 4B). Those residual undifferentiated cells might be responsible for the formation of teratomas in the recipients.

To prevent teratomas from forming in recipients, we purged SSEA-4$^+$ cells of the putative hematopoietic precursors and transplanted the SSEA-4$^-$ population into the fetal monkey liver ($n = 6$) (Fig. 4C). At delivery, tumors were no longer observed in the six animals that had been transplanted with the sorted SSEA-4$^-$ cells (Fig. 4D). The transplanted cell-derived CFU were clearly detected in the newborns, and